ICARUS 82, 111–145 (1989)

Transitional Morphology in West Deuteronilus Mensae, Mars: Implications for Modification of the Lowland/Upland Boundary

TIMOTHY J. PARKER, R. STEPHEN SAUNDERS, AND DALE M. SCHNEEBERGER*

Jet Propulsion Laboratory, California Institute of Technology, 4800 Oak Grove Drive, Pasadena, California 91109

Received June 27, 1988; revised January 20, 1989

West Deuteronilus Mensae, which lies along the lowland/upland boundary of Mars at 45° latitude, 345° longitude, exhibits both gradational (L. A. Rossbacher, 1985, in *Models in Geomorphology* (Woldenberg, Ed.), pp. 343–372, Allen & Unwin, Boston) and fretted terrain (R. P. Sharp, 1973, *J. Geophys. Res.* 78, 4073–4083) boundary types. To the west, the boundary is gradational and to the east it is defined by fretted terrain. The two types of boundaries do not merge with one another within the west Deuteronilus Mensae region, however. The gradational boundary materials appear to overlap the fretted terrain by about 500 km. Contacts between units associated with the gradational boundary and the fretted terrain boundary can both be recognized in the region of overlap. The fretted terrain can be identified as much as 300 km north of the gradational boundary in this region. Lowland units associated with the gradational boundary embay canyons of the fretted terrain in a topographically conformal fashion. Changes in the fretted terrain across the gradational boundary (from uplands to lowlands) include a reduction of canyon wall slopes and depths, such that the fretted terrain north of the gradational boundary appears mantled but not obscured. There are at least two major classes of processes which might explain the lateral overlap: (1) erosion of stratified upland terrain and (2) deposition of plains materials onto the sloping upland margin and fretted terrain. Erosion of stratified upland terrain does not adequately explain the plainward decrease in crater densities across the gradational boundary nor is it consistent with evidence that lowland plains material appears to onlap the sloping upland margin in several places. Of the possible plains emplacement mechanisms, eolian deposition would not produce the sharp, apparently topographically conformal gradational unit contacts. Volcanic plains emplacement would not preserve the complex geometry of the underlying fretted terrain. Sediment deposition in either a liquid or ice-covered sea could produce the draped appearance of the fretted terrain. Outflow channels along the lowland/upland boundary, particularly those of the circum-Chryse and west Elysium regions, may have flooded the northern lowlands to depths of tens to hundreds of meters. The gradational unit contacts may represent the shorelines of such a sea. The scale of characteristic morphologies along these contacts may require an unfrozen condition of sufficient duration to allow lacustrine-style wave erosion and redistribution of material along the contacts. Our limited understanding of the Martian paleoclimate and H_2O inventories allows the possibility of clement periods in the past, and other geological evidence (e.g., small valley networks and outflow channels) strongly suggests an extensive role of liquid water.

INTRODUCTION

The northern lowlands of Mars are separated from the southern uplands by a prominent topographic boundary (Carr 1986,

* Present address: SNR Company, Inc., Geotechnical and Environmental Consultants, 25301 Cabot Road, Suite 212, Laguna Hills, California 92653.

0019-1035/89 $3.00

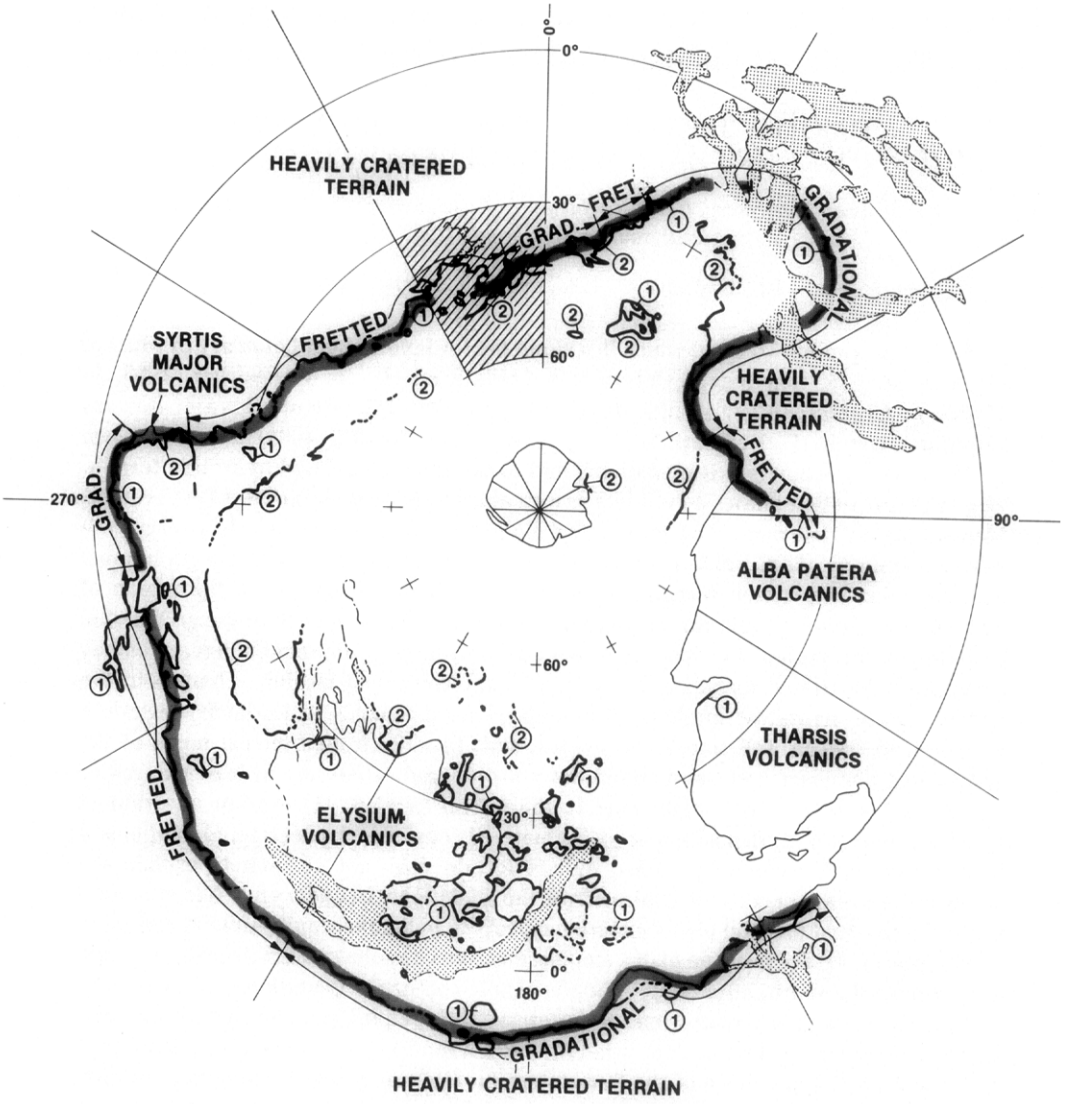

FIG. 1. Polar projection of northern lowland plains of Mars relative to major bounding provinces (adapted from Scott and Tanaka 1986, Greeley and Guest 1987, Tanaka and Scott 1987, and indicated by thin black lines). General location of lowland/upland boundary is indicated by a broad gray line (adapted from Scott and Tanaka 1986, Greeley and Guest 1987). The two principal types of lowland/upland boundary are indicated as either "gradational" or "fretted." Major outflow channels are indicated by stippled areas and by alternate dot–dashed thin black lines. Global distribution of unit boundaries described in the text is indicated by heavy black lines labeled 1 and 2 (dashed where positive identification is limited by available image resolution). Contact No. 1 separates cratered uplands from lowland unit A. Contact No. 2 separates lowland unit A from lowland unit B. Location of the Ismenius Lacus Quadrangle (Fig. 2) is indicated by a diagonal pattern.

Lucchitta 1984a, Mutch *et al.* 1976, Scott and Carr 1978, Squyres 1978, 1979). Locally this boundary is defined by two principal types (Fig. 1). In the first type of boundary, described by Rossbacher (1985) as "gradational," the cratered uplands dip gently northward into the lowland plains over several tens of kilometers and appear onlapped by plains materials along a distinct contact (Carr 1981, Rossbacher 1985). Placement of the lowland/upland boundary by Scott and Carr (1978), Scott and Tanaka

(1986), and Lucchitta (1978) corresponds, for the most part, with this contact. A second contact, delineating a transitional plains surface between the first contact and the bulk of the northern plains, in most cases lies a few tens of kilometers plainward of the first contact (Fig. 1). The gradational boundary is best expressed in southwest Chryse Planitia, along the northeast margin of Tempe Terra, in southeast Acidalia Planitia, and in southern Isidis Planitia.

In the second type of lowland/upland boundary, termed fretted terrain (Sharp 1973), a pronounced escarpment clearly separates lowlands from uplands and suggests erosion of the upland material at the cliff face (Carr 1981, 1984, Sharp 1973). Fretted terrain occurs in two major belts along the lowland/upland boundary separated by the Isidis Basin and along the northwest margin of Arabia Terra in Cydonia Mensae (30 to 40° latitude, 10 to 20° longitude). Mareotis Fossae (40 to 55° latitude, 65 to 85° longitude) also exhibits fretted terrain morphology to some extent, though it is likely more tectonic than erosional in origin. The fretted terrain northwest of Isidis is defined by the Deuteronilus–Protonilus–Nilosyrtis Mensae system (30 to 50° latitude, 280 to 350° longitude). East of Isidis lies the Nepenthes–Aeolis Mensae system (210 to 260° longitude, −10 to 15° latitude). The difference in gross morphology between these regions is largely due to the greater topographic separation between uplands and lowlands at the fretted terrain escarpments northwest of Isidis than is observed to the east. The fretted terrain of both regions exhibits a complex transition zone consisting of upland plateau and knob outliers and lowland plains reentrants. This transition zone may be several hundred kilometers wide in places.

Because the two principal boundary types are so different morphologically and perhaps genetically, their relationship is important in understanding how the lowland/upland boundary evolved globally. Characterizing the relationship between the two boundaries requires evidence of lateral continuity from one boundary type to the other or superposition of surface units associated with one boundary type by those of the other. It should be pointed out, however, that the genesis of the two boundaries may be relevant only to the late development of the lowland/upland boundary, rather than to the origin of the crustal dichotomy itself. We are concerned here with characterizing the lateral transition from a gradational boundary to a fretted terrain boundary and its geologic implications, rather than with the origin of the planetary dichotomy. Six major occurrences of lateral transition from a fretted terrain to a gradational boundary are noted, including northeast of Mareotis Fossae, southwest and northeast of Cydonia Mensae, west of Deuteronilus Mensae, east of Isidis Basin, and east of Aeolis Mensae (Fig. 1). For this characterization, we will examine the west Deuteronilus Mensae region (Figs. 2 and 3) as it exemplifies this lateral change and is well covered by high-resolution Viking Orbiter images.

The lateral change from a gradational to a fretted terrain boundary in west Deuteronilus Mensae is expressed by the apparent overlap of the fretted terrain by the upland and lowland surfaces associated with the gradational boundary for hundreds of kilometers. Plains units embay canyons of the fretted terrain. The fretted terrain appears subdued north of the gradational boundary, yet it is still easily recognized. Development of this lateral overlap may have at least two plausible origins. First, unit contacts associated with the gradational boundary might represent stratigraphic contacts exposed through erosional development of the fretted terrain and sloping upland margin. This erosion might include scarp retreat through thermokarstic removal of interstitial ice (e.g., Carr and Schaber 1977, Guest *et al.* 1977, Rossbacher 1985, Weiss *et al.* 1981). Second, the apparent overlap of the fretted terrain by units associated with the gradational boundary might indicate emplacement of plains materials onto the northward-dipping plateau surface and fretted terrain.

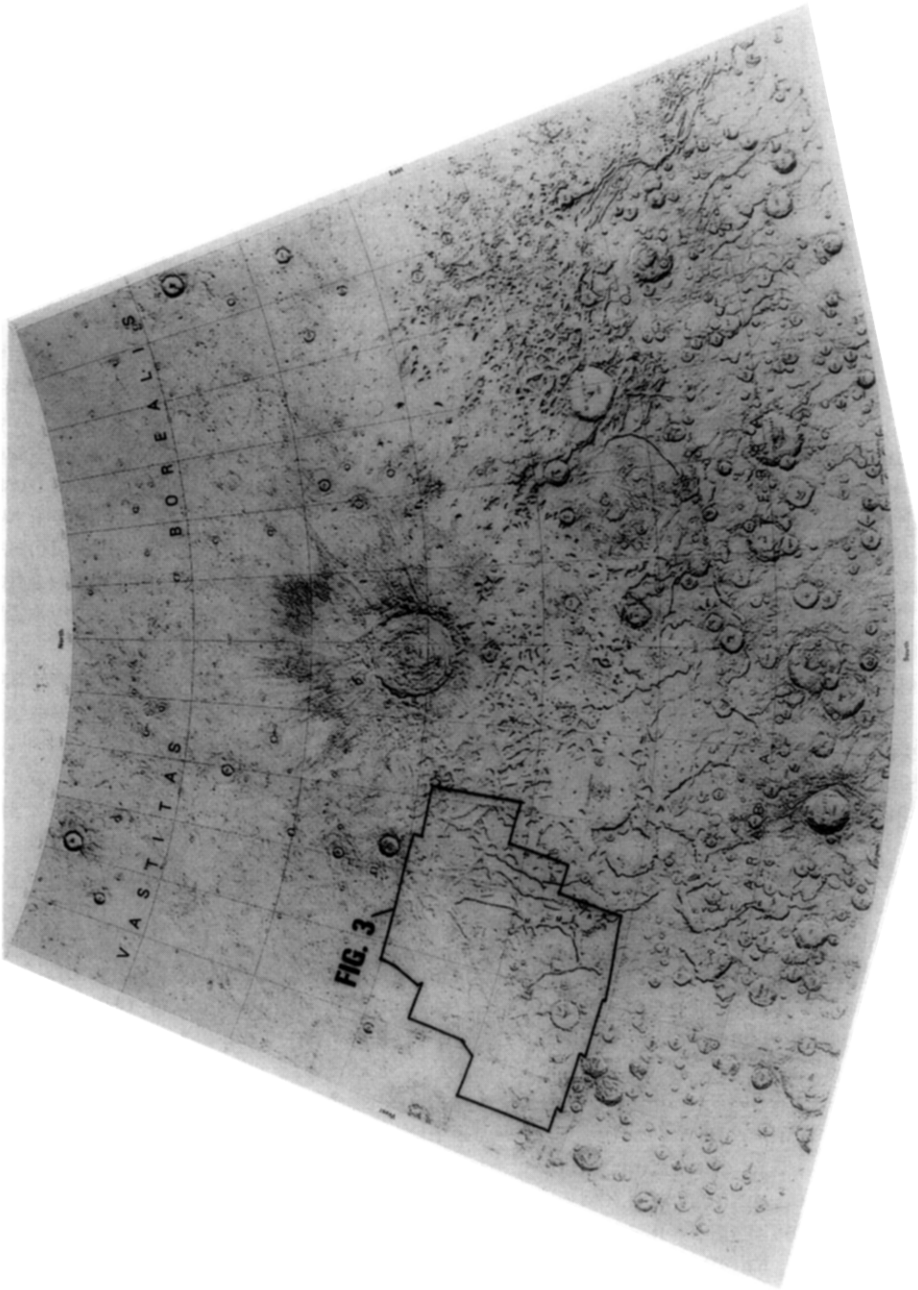

FIG. 2. Shaded relief map of the Ismenius Lacus Quadrangle of Mars. The lowland/upland boundary runs from east to west through the quadrangle. Regional downslope is to the north. Study area (Fig. 3) is indicated. Gradational lowland/upland boundary changes to Fretted Terrain boundary from west to east in this area. USGS Map I-1495, 1:5,000,000 Series.

Several mechanisms of emplacement of plains materials in the northern lowlands, through volcanism or sediment deposition, have been postulated. Volcanic plains emplacement processes include large-scale basaltic flood volcanism (e.g., Carr 1981, Theilig and Greeley 1979) or flood volcanism onto ice-rich substrates (Frey *et al.* 1979, Frey and Jarosewich 1982). Sedimentary plains emplacement mechanisms include eolian deposition (Grizzaffi and Schultz 1987, Soderblom *et al.* 1973) or outflow channel deposition either subaerially (e.g., McGill 1985, 1986, Lucchitta *et al.* 1986) or into an ice-covered standing body of water (Lucchitta *et al.* 1986). In this paper, we propose that sediment deposition within a standing body of liquid water warrants careful consideration. Lacustrine or shallow marine erosion and deposition may provide explanations for specific morphologic elements of the lowland/upland boundary that are inadequately accounted for by other processes.

METHODOLOGY

In the following section, the lateral overlap of the fretted terrain by units associated with the gradational boundary in west Deuteronilus Mensae is examined. Emphasis is placed on the characterization of morphological changes across the gradational boundary of the fret canyon centered at 46° latitude, 346° longitude, since it is well covered by both medium-resolution (approximately 200 m/pixel) and very-high-resolution (9–11 m/pixel) images. This includes local and regional topographic information as well as physical descriptions of specific morphologies. Comparisons are then made between the regional distributions and morphologies of the surface units associated with the gradational boundary in the medium- and high-resolution (approximately 50 m/pixel) images.

Canyon depths south of about 46° latitude were determined from shadow measurements using Viking Orbiter image 673B43, which has a resolution of 204 m/pixel and a Sun elevation of 9° above the horizon. An error in shadow determination of two pixels (corresponding to a vertical error of ±64 m) was assumed to account reasonably for rounding of either the top or the base of the slope and for errors in determining the exact location of shadow margins. The actual errors introduced by rounding of the slope should be least where the slopes are steep, and greatest where the slopes are gentle. North of about 46° latitude, rounding of the top and base of the slope appears so significant that photoclinometric profiles were considered more reliable than shadow measurements. A symmetrical model, which determines the albedo of a symmetrical feature (such as a crater, or in this case a canyon) from the lighting geometry relative to the brightness of the up- and down-Sun sides of the feature, was used to generate these profiles. The profiles were acquired from Viking Or-

FIG. 3. (a) Computer mosaic of southwest Deuteronilus Mensae compiled from 78 Viking Orbiter images. Medium-resolution (~200 m/pixel) images: 675B32, 34, 36, 52, 54–59. High-resolution (50–70 m/pixel) images: 52A34-52, 60A49, 51-60, 61A11-13, 15-30. Very-high-resolution (9–11 m/pixel) images: 458b45-51, 61-72. (b) Generalized geomorphic map of study area. Regional downslope is toward the north northwest at the center of the figure. The contact between the cratered uplands and lowland unit A is easily identified crossing plateau surfaces in the fretted terrain. Its position within the fret canyons cannot be determined with certainty at medium resolution, however. Based on the very-high-resolution images (see Fig. 4) and for the sake of simplicity, however, fret canyon floors and debris aprons are included within lowland unit B. The contact between lowland units A and B is traceable throughout the west Deuteronilus Mensae region, interrupted only by relatively fresh impact craters and ejecta blankets. This contact crosses plateau outliers and fret canyon floors. Shading across at least two of these canyon floor crossings (at C and D) suggest that the contact may be defined by a narrow ridge. Striped and Mottled Plains are subunits of lowland unit B. Narrow, closely spaced rills are indicated at R. Footprints for subsequent figures are indicated with labeled boxes.

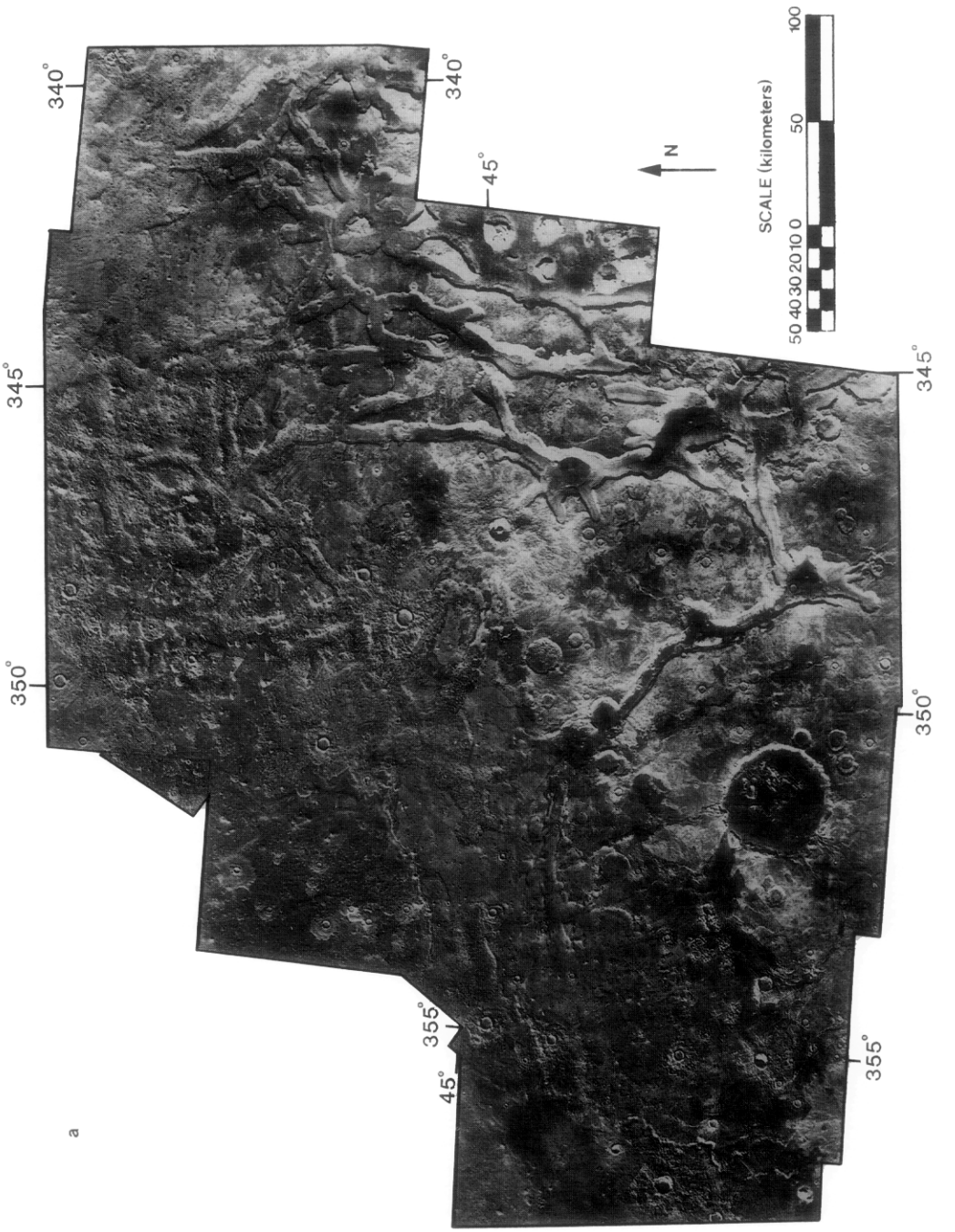
340°
340°
45°
N
SCALE (kilometers)
50 40 30 20 10 0 50 100
345°
345°
350°
350°
355°
355°
45°
a


340°
340°
345°
345°
350°
350°
355°
355°
45°
45°
LOWLAND UNIT B
LOWLAND UNIT A
CRATERED UPLANDS
SMOOTH PLAINS
HILLY AND KNOBBY PLAINS
LOWLAND UNIT B
LOWLAND UNIT A
N
SCALE (kilometers)
50 40 30 20 10 0 50 100
b

biter image 675B59, with a resolution of 198 m/pixel and a Sun elevation of 22° above the horizon. Additional photoclinometric profiles were obtained from the very-high-resolution (9–11 m/pixel) images of orbit 458B. Since only one side of the fret canyon is covered by these images, an asymmetric model was used. In this method, a flat field D.N. value was derived from the plateau surface. The asymmetric model assumes a uniform albedo for the entire profile, however, so the high-resolution profiles were used for qualitative comparison with the low-resolution symmetric profiles in supporting visual estimates of the shape of specific slope elements rather than quantitative depth values. Between about 44 and 46° latitude, shadow measurements taken from Viking Orbiter image 673B43 and photoclinometric profiles taken from Viking Orbiter image 675B59 could be compared to one another. Values for the total depth of the canyon derived by both methods agree to within 20%.

Crater distributions for the three photogeologic units associated with the gradational boundary were derived by counting all recognizable craters within each unit and then separating individual crater populations using the technique of Neukum and Hiller (1981). Identification during the counting phase of "fresh" (i.e., those craters that clearly postdate a given surface) versus degraded crater populations would be the preferred method of separating the various populations (e.g., Maxwell and McGill 1988, Tanaka 1986). But, because of the wide range in image resolution from which these data were acquired, and because we were dealing with crater diameters that are typically smaller than those counted by other investigators, we felt that it would not be possible to make a clear separation. We found that many craters that appeared "fresh" at 200 m/pixel might appear modified at 50 m/pixel, and most showed evidence of degradation at 10 m/pixel.

In the Neukum and Hiller (1981) technique, individual crater populations are identified on a plot of the derivative of the cumulative plot for each unit. "Plateaus" in the original cumulative plot have positive slopes on the derivative cumulative plot, making them more apparent. Each separate population curve is then compared to the Mars Standard crater curves of Neukum and Hiller (1981) and Neukum (1983) to determine the crater retention age of each resurfacing event. This value is presented as the cumulative number of craters greater than or equal to a given diameter per million square kilometers. The reliability of the crater ages derived via this technique is subject to the placement of the diameter break between individual populations. Interpretations based on crater populations acquired in this way must therefore be made with caution.

The Neukum (1983) curve is much flatter in the diameter range 2–20 km than the Neukum (1981) curve, so crater numbers derived by fitting to the 1983 curve are lower than those derived by fitting to the 1981 curve for populations that include craters greater than 2 km in diameter. Also, since the Neukum (1983) curve is flatter it is not always necessary to separate populations in this range to get a reasonable fit to the production curve, even though the break may appear distinct on the derivative cumulative plot. In general, however, we found that the Neukum and Hiller (1981) production curve tended to provide a better fit to our crater data in the diameter range 2–20 km than did the Neukum (1983) curve.

GEOMORPHIC ELEMENTS

Overlap of the fretted terrain by lowland plains units north of the gradational boundary suggests that the upper surfaces of some plateau outliers may be composed of lowland plains materials. This may appear to be a contradiction in terminology. The terms "upland" and "lowlands" are generally applied in the literature in a regional sense to indicate surfaces to either side of the planetary dichotomy. For the purpose

of this discussion we will adhere to the clear separation of upland and lowland surfaces exemplified by the gradational boundary west of Deuteronilus Mensae and designate all surfaces to the north as lowland surfaces, to the extent that the gradational boundary can be identified in the fretted terrain within Deuteronilus Mensae.

Surfaces associated with the gradational lowland/upland boundary southwest of Deuteronilus Mensae can be divided into three principal photogeologic units (one cratered upland unit and two northern lowland units) with differences in morphology and crater densities. We will refer to these surfaces as cratered uplands, lowland unit A, and lowland unit B.

Gradational Boundary

Cratered Uplands

General description. The cratered uplands have a varied albedo that, on average, is higher than that of lowland unit A to the north. In very-high-resolution images (Fig. 4) the cratered uplands appear to have a texture generally rougher than that of lowland unit A. Wrinkle ridges are common and trend north to northwest, similar to the orientation of many of the fret canyons in the region. Small valley networks are common in the cratered uplands outside the study area. A few shallow, branching networks only a few hundred meters wide and few tens of kilometers long can be seen on isolated plateau remnants on the east side of Fig. 3. These small valleys terminate at the contact between the cratered uplands and unit A. An unnamed outflow channel also terminates at the contact between the cratered uplands and unit A within the 75-km crater Semeykin and west of Semeykin (at 42° latitude, 353° longitude). This is a shallow channel up to 30 km or more wide and over 400 km long that appears to originate in an intercrater region at approximately 35° latitude, 349° longitude (Fig. 2).

Crater ages. Three crater populations have been identified within the cratered uplands using the Neukum and Hiller (1981) technique (Fig. 5). The oldest, most distinct population consists of craters between about 5 and 30 km in diameter. This population corresponds well with a Mars Standard curve with a crater retention age between about 25,000 and 35,000 (population 1, Fig. 5). This places the unit in reasonable agreement with crater ages derived by other investigators for surfaces associated with the lowland/upland boundary (e.g., Frey and Semeniuk 1988, Frey *et al.* 1986, Grant and Frey 1988, Grant *et al.* 1988). The remaining two populations indicate limited resurfacing events, affecting craters less than 5 km in diameter, that ended at crater ages from about 3200 to 7000 and from 1700 to 2400 (populations 2 and 3, Fig. 5). In fitting the data to the Neukum (1983) production curve, populations 1 and 2 were not separated, giving a retention age of 7000–15,000 for the combined plot. Population 3 has the same Neukum and Hiller (1981) and Neukum (1983) crater retention age because the two production curves are essentially the same for craters smaller than about 2 km in diameter.

The lower part of the curve for populations 1 and 2 (craters from population 1) is noticeably steeper than the Neukum (1983) curve, yet fits the slope of the Neukum and Hiller (1981) curve well. It is easier to explain a population curve slope that is flatter than the crater production curve (through more advanced degradation of smaller craters than large ones) than it is one that is steeper than the production curve (possibly requiring reevaluation of the production curve). For this reason, we feel that the Neukum and Hiller (1981) curve provides a more realistic fit.

Contact with lowland unit A. The cratered uplands are separated from lowland unit A by the sharp, irregular contact that defines the gradational lowland/upland boundary. Locally, this contact is deflected southward into topographic lows, such as the crater Semeykin and the fret canyons, such that the plains material appears to em-

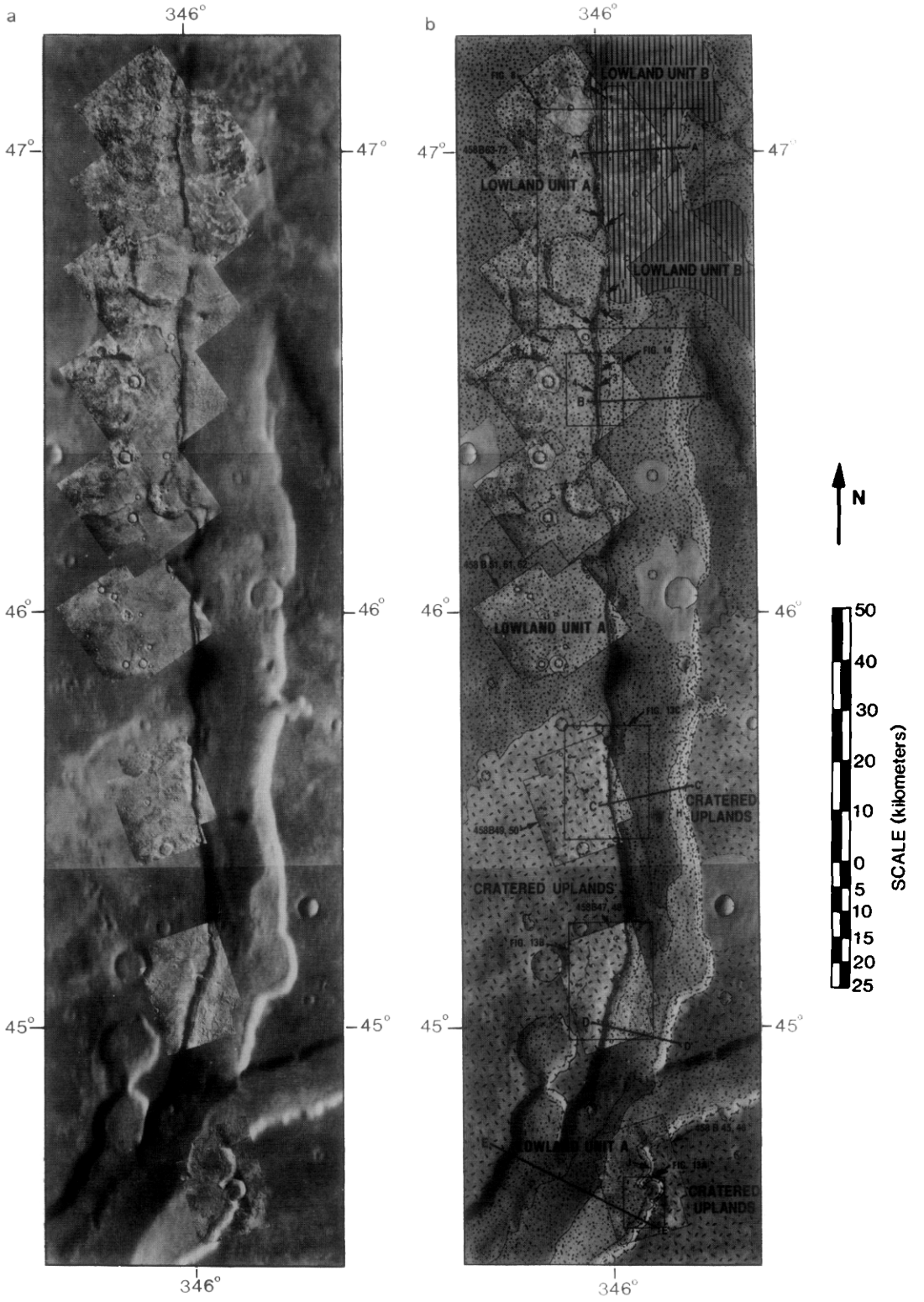
a
b
346°
47°
46°
45°
LOWLAND UNIT B
LOWLAND UNIT A
CRATERED UPLANDS
N
SCALE (kilometers)
50
40
30
20
10
0
5
10
15
20
25

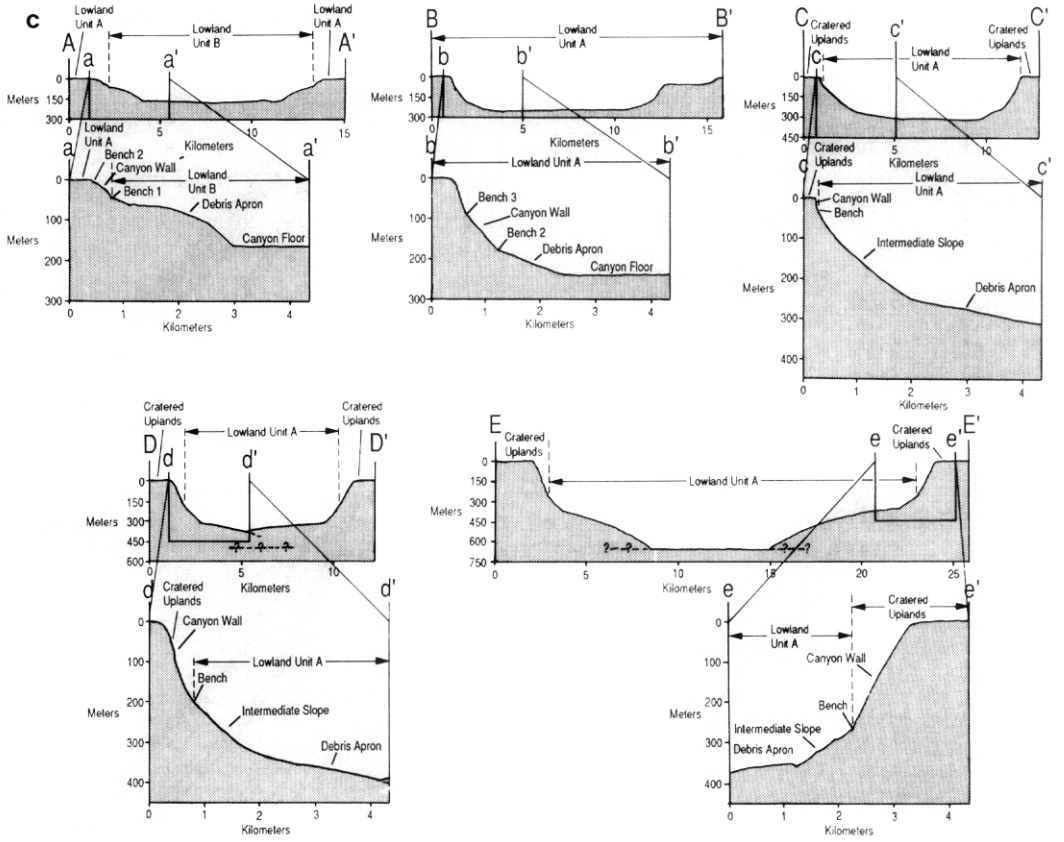

FIG. 4—*Continued*

bay the cratered uplands. High-resolution coverage of this contact is limited, but where it is available, evidence for both onlapping of the cratered uplands by the plains material and erosion of the cratered uplands at the contact can be seen (Fig. 6).

Lowland Unit A

General description. Lowland unit A is equivalent to the smooth plains unit mapped by Rossbacher (1985) in southeast Acidalia Planitia. It has an albedo distinctly

FIG. 4. (a) Computer mosaic of medium- and very-high-resolution images of fret canyon at 46° latitude, 346° longitude (see Fig. 3 for location). (b) Generalized geomorphic map of fret canyon. Regional downslope is to the north. The escarpment separating lowland unit A into a northern polygonally patterned and a smooth southern surface is indicated at F. A similar, though less prominent, feature, parallel to and midway between this escarpment and the contact between the cratered uplands and lowland unit A is indicated at G. The northern limit of prominent debris aprons is shown at H. Benches and breaks in slope identified in the very high resolution images are numbered 1–4, from topographically lowest to highest. An additional break in slope, not numbered, separates the cratered uplands and lowland unit A on the canyon's west wall. A break in slope on the east side of the canyon, at J, may be the expression of the contact between the cratered uplands and lowland unit A on this side of the canyon. (c) Schematic cross-profiles of fret canyon based on shadow measurements and photoclinometry. Full-canyon profiles (uppercase letters) are based on medium-resolution images. Inset profiles (lowercase letters) are based on comparison of medium-resolution data with photoclinometry of very-high-resolution images. Contacts between surface units relative to canyon profiles are indicated by vertical dashed lines and labeled. Vertical exaggeration is approximately 7 times.

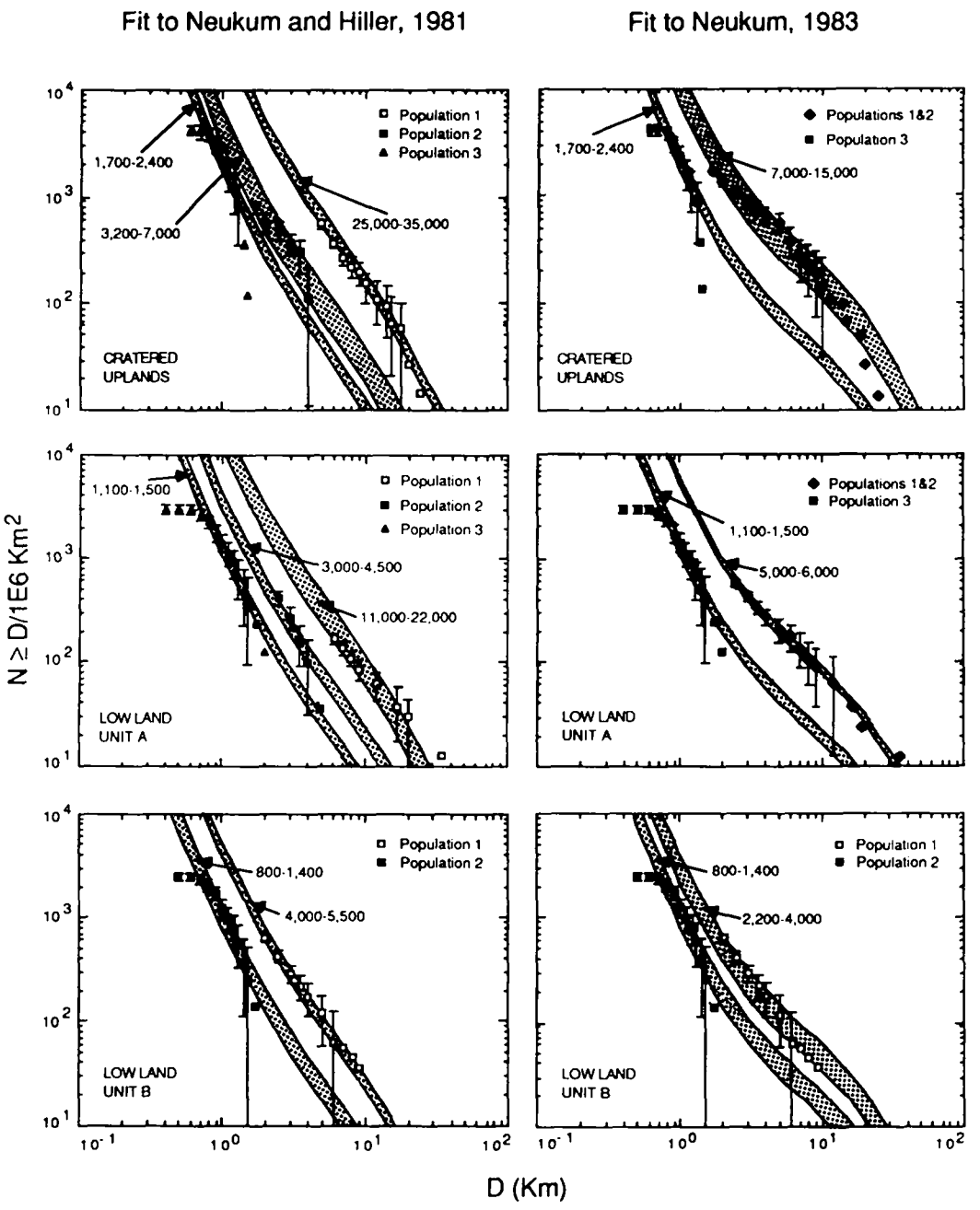

FIG. 5. Cumulative crater size–frequency curves for the cratered uplands and lowland units A and B. Data were binned using the technique of Neukum and Hiller (1981) and compared to their Mars Standard curve (left column) and that of Neukum (1983) (right column) to determine the crater retention age (cumulative number of craters greater than or equal to a given diameter/million km^2) of resurfacing events. Total cumulative plots (not separated into multiple populations) reflect a pronounced plainward decrease in crater density with maximum retention ages given by the oldest populations for each unit. Area of cratered uplands = 74,208 km^2. Area of lowland unit A = 81,230 km^2. Area of lowland unit B (including both "striped" and "mottled" plains subunits) = 109,578 km^2.

FIG. 6. High-resolution coverage of contact between cratered uplands and lowland unit A (see Fig. 3 for location). Lowland unit A appears to onlap cratered uplands at A. At B, however, there is a recognizable escarpment in the cratered upland margin, suggesting erosion of the cratered upland material locally. Scene width, approximately 70 km. Unless otherwise noted north is toward the top of the frame. Viking Orbiter images: 61A19,20.

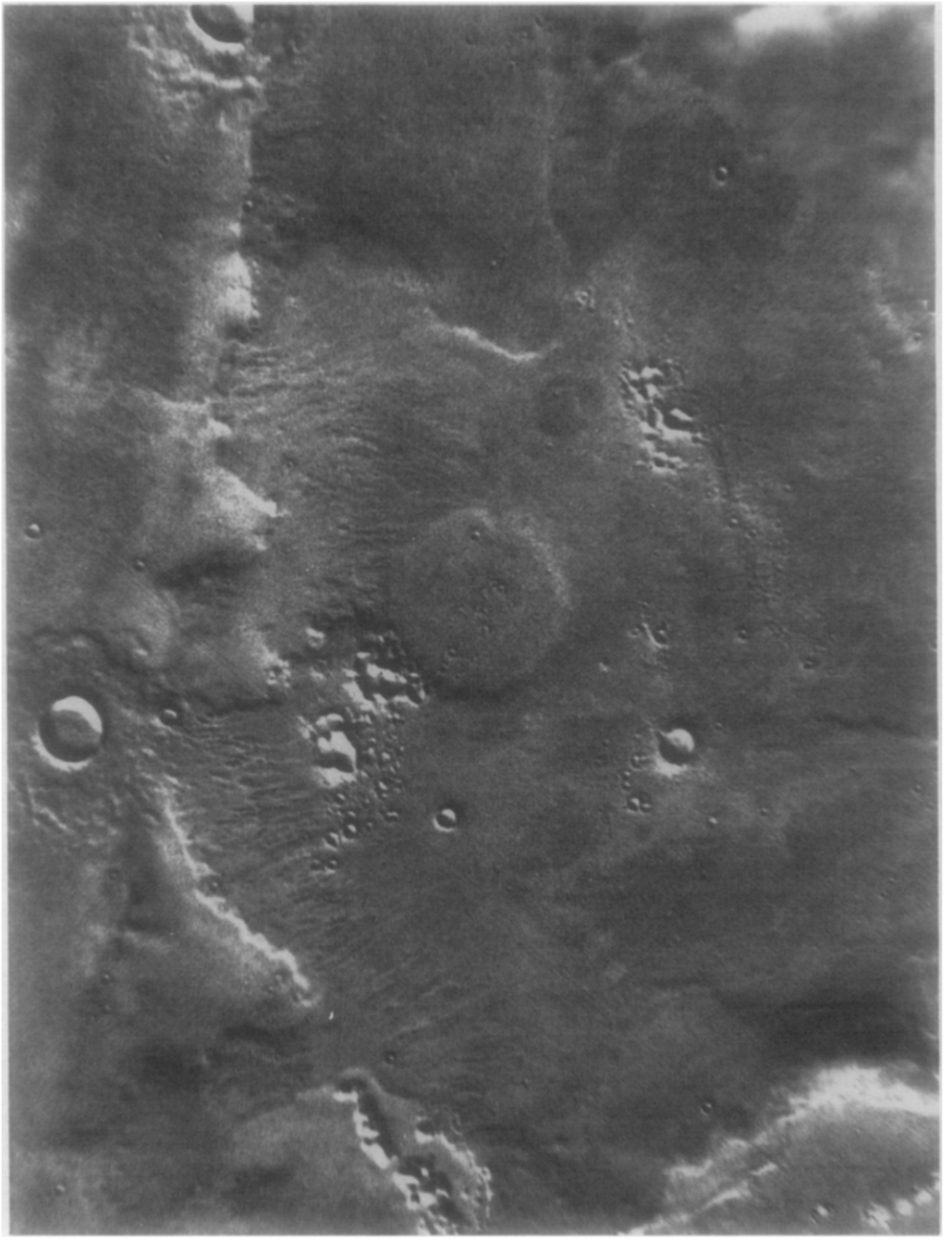

FIG. 7. High-resolution images of closely spaced, narrow rills within lowland unit A (see Fig. 3 for location). Individual rills are shallow, nonbranching valleys less than a few hundred meters wide. Scene width, approximately 50 km. Viking Orbiter images: 61A27,29,30.

lower and more uniform than that of the cratered uplands (Figs. 3 and 4). Wrinkle ridges are less numerous in unit A than in the cratered uplands. Shallow, branching small valley networks are absent. Instead, a system of closely spaced rills (Fig. 7) is present on many of the plateau remnants in west Deuteronilus Mensae east of the fret canyon in Fig. 4 (Fig. 3). They are also found in a band 5–10 km wide from 45° latitude, 349° longitude, southwest for about 250 km to 43° latitude, 352° longitude (Fig. 3). These rills are very narrow (typically less than 200 m wide) and nonbranching and are oriented perpendicular to the general trend of the lowland/upland boundary and regional topography. This orientation seems to predominate, though there does appear to be some local topographic control in places (i.e., at plateau margins). The rills are very sharply defined relative to the fret canyons, and are lightly cratered, suggesting that they postdate the fretted terrain.

At least two nonbranching, or stem, valleys (Pieri 1980) lie within unit A at 45° latitude, 349° longitude, and at 43° latitude, 357° longitude (Fig. 3). These are deeply entrenched valleys a few kilometers wide. The westernmost of these is over 150 km long and is covered by the high-resolution images, in which it appears softened or mantled by unit A.

In very-high-resolution images, surface textures suggest lowland unit A may be divisible into two subunits. In Fig. 4 these surfaces are separated by an east–west trending escarpment. The surface south of this escarpment is characterized by its distinctly smooth texture and relatively uniform albedo. The surface north of the escarpment has a more mottled appearance. Its most notable characteristic is the presence of well-defined polygons several tens of meters to as much as 300 m across (Fig. 8) (Lucchitta 1984b). Similar, though somewhat larger, polygons can be seen in high-resolution images more than 200 km to the southeast (Fig. 9). These lie in the same position relative to the unit contacts as do those in Fig. 4, and may indicate regional continuity of this surface.

The escarpment separating the two surfaces can be traced in the medium-resolution images for about 50 km west of the fret canyon in Fig. 4, and appears to parallel the contacts between the cratered uplands and unit A and between units A and B. At least one other feature exhibiting this parallel aspect is a narrow, irregular albedo feature (Fig. 4). The unit A surfaces on either side of this feature do not seem to differ significantly at this scale, though the northern surface may have a slightly higher albedo.

Crater ages. Three crater populations were identified within lowland unit A. Craters larger than about 10 km in diameter are rare. Most of those counted are highly degraded ghosts. These correspond to a Neukum and Hiller (1981) Mars Standard curve with a crater retention age between 11,000 and 22,000 (population 1, Fig. 5), and likely represent a remnant of population 1 of the cratered uplands plot that was not completely obliterated by formation of unit A. Populations 2 and 3 (Fig. 5), correspond to Neukum and Hiller (1981) crater retention ages from 3000 to 4500 and from 1100 to 1500, respectively. Population 2 appears to be essentially the same age as population 2 of the cratered uplands plot, while population 3 appears slightly younger than population 3 of the cratered uplands. When compared to the Neukum (1983) curve, populations 1 and 2 together provide a good fit to a retention age between 5000 and 6000 (Fig. 5). This may be a coincidence, however, because many of the craters in population 1 are degraded ghosts and should exhibit a flatter cumulative plot than a fresh population would.

Contact with lowland unit B. The contact between lowland units A and B can be easily traced across the entire region in Fig. 3, interrupted only by relatively fresh impact craters and ejecta blankets. Though it may correspond approximately to low escarpments in places (Carr and Schaber 1977, Rossbacher 1985), it can be traced across

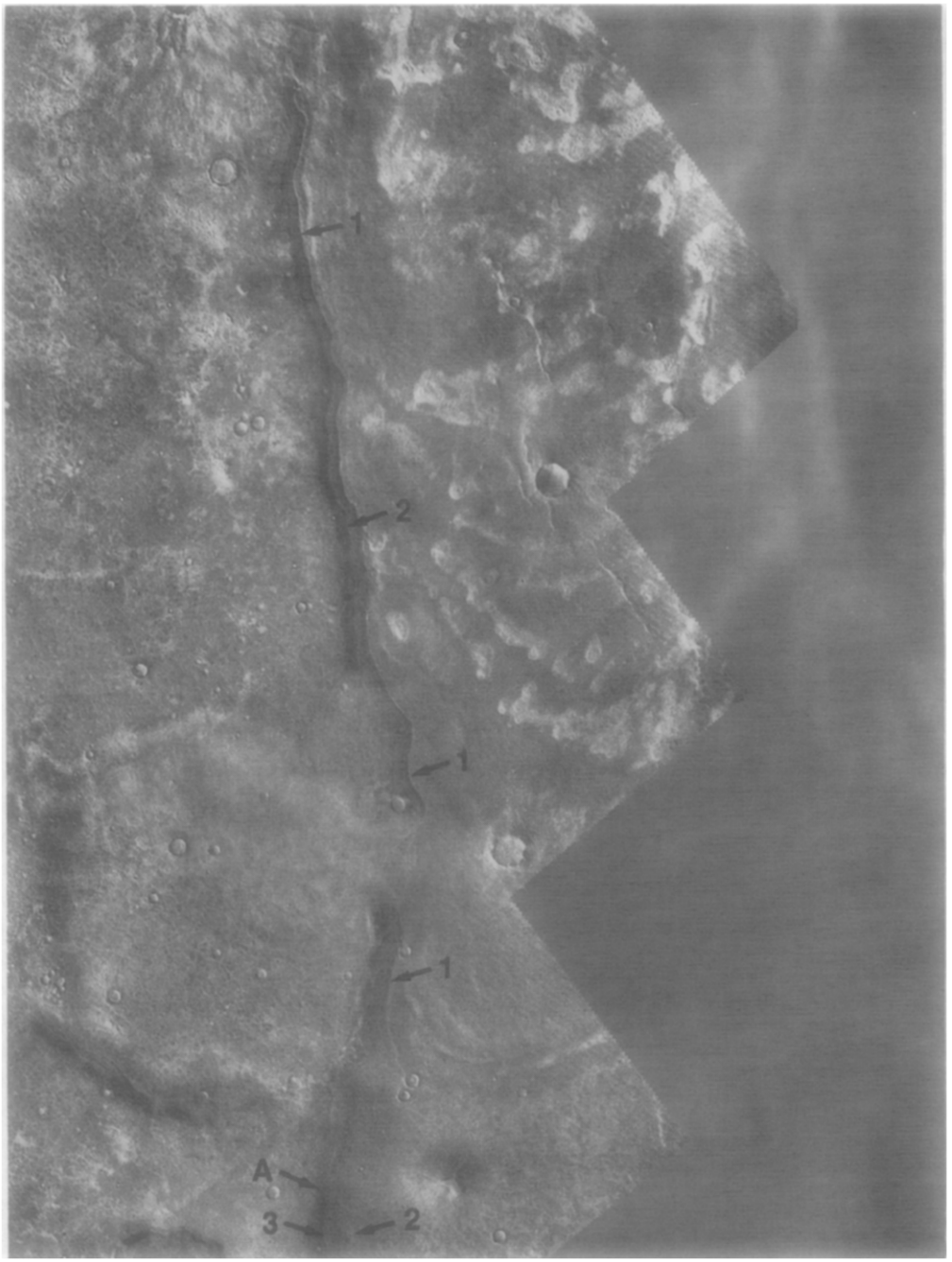

FIG. 8. Very-high-resolution coverage of lowland units A and B on west side of fret canyon (see Fig. 4 for location). The northern surface of unit A is characterized by polygons several tens to ~300 m across (at left). Similar, though somewhat larger, polygons are visible on the canyon floor south of the contact between lowland units A and B and may indicate a topographically conformal offset of the surface on the canyon floor. Note the mantled appearance of the 10-km degraded crater by the polygonally patterned surface. A striped or "thumbprint" texture of lowland unit B is revealed in the very-high-resolution images as disconnected arcs of bright, low-relief mounds (at center). Benches and breaks in slope on the canyon wall are numbered 1–3. Bench 2 intersects the top of the wall near the

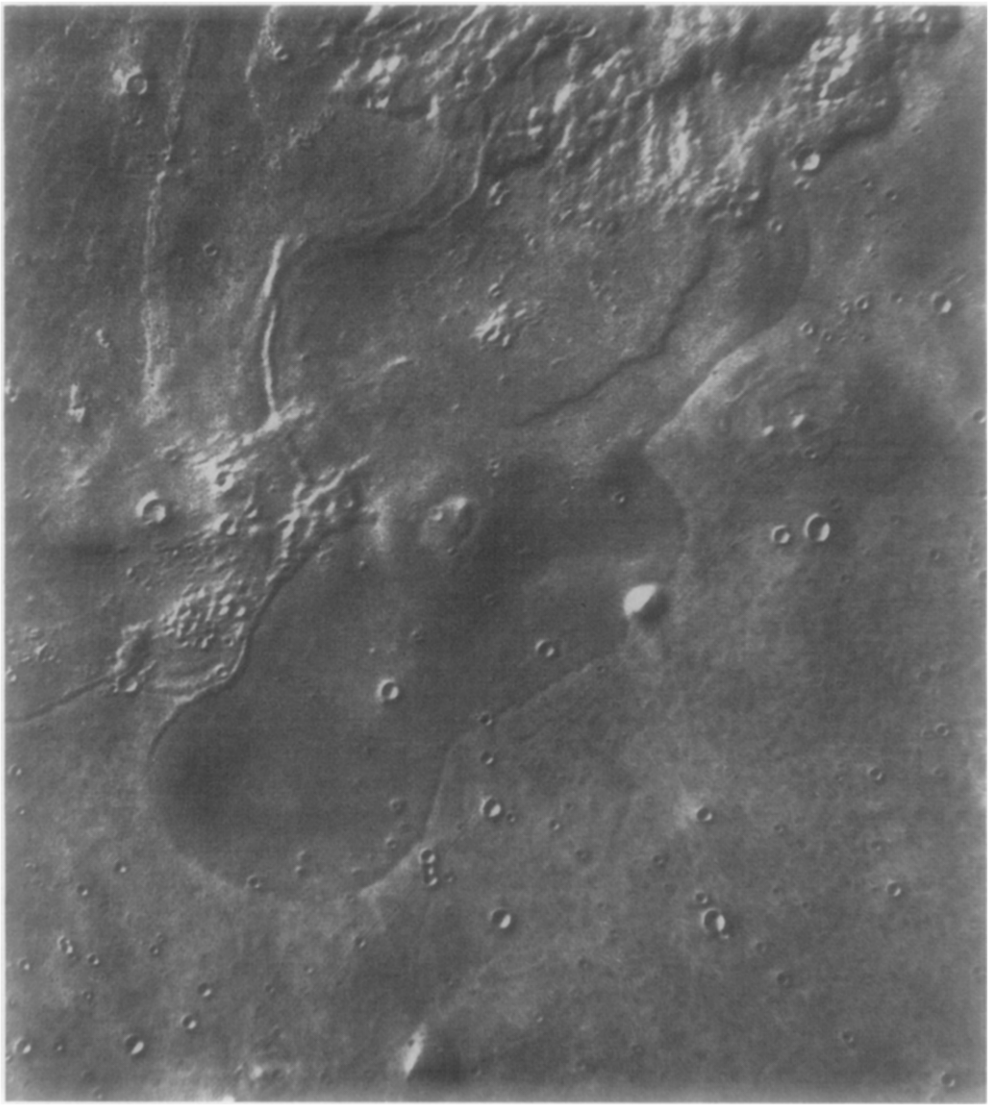

FIG. 9. High-resolution coverage of lobate contact between lowland units A and B (see Fig. 3 for location). Polygons similar to but larger than those to the east are recognizable at lower right. Scene width, approximately 35 km. Viking Orbiter images: 61A21,22,24.

top of the frame. Bench 3 intersects the top of the canyon wall just south of the 10-km degraded crater. Bench 1 is the only one of the 3 that intersects the canyon floor in the very-high-resolution images, where it defines the contact between lowland units A and B. The gentle ridge-and-swale structure along this contact grades into bench 1 at the base of the canyon wall. Shading immediately above benches 1 and 2 suggests that the steepest slopes are above, rather than below, each bench, opposite the profile shape typical of stratigraphic benches. Canyon wall slopes here probably average close to 6°, making preservation of well-defined stratigraphic benches unlikely. Scene width, approximately 25 km. Viking Orbiter images: 458B65-70.

FIG. 10. High-resolution coverage of plateau outliers surrounded by striped terrain (see Fig. 3 for location). The regional slope is down to the northwest. Higher plateau surfaces consist of lowland unit A material. Contact between lowland units A and B on small plateaus at lower left appears to onlap the upper surface of each, particularly on their north and west sides. This contact also onlaps the larger, roughly triangular plateau outlier (center), though much more extensively on its north and west sides and appears to embay a shallow depression at A. Scene width, approximately 80 km. Viking Orbiter images: 52A43-46, 60A55,58-60.

plateau outliers (Figs. 3 and 10) and fret canyon floors (Figs. 3, 4, 8, and 11) as well. Where it crosses the canyons, it exhibits a smooth, lobate or arcuate pattern concave down-canyon. These arcs can be identified in several fret canyons. In at least two places, shading along the contact suggests the arcs may be defined by a narrow ridge (Fig. 3). In very-high-resolution images, another of these arcs appears to consist of a system of parallel, low-relief ridges and swales (Fig. 8).

Lowland Unit B

General description. Lowland unit B is equivalent to the hummocky cratered plains unit mapped by Rossbacher (1985) in the southeast Acidalia Planitia region. No small valley networks occur within lowland unit B in the study region. In the high-resolution images, unit B can be divided into two subunits (Figs. 3 and 12). The southern subunit consists of the striped or "thumbprint" terrain described by Guest *et al.* (1977). The prominent striping effect is due to a system of bright, low-relief mounds or pits viewed against relatively dark, smooth plains. In places these mounds are distributed in parallel arcs (Fig. 8). They are most pronounced in fret canyon reentrants in the east half of Fig. 3, where they are arranged with their concave sides facing down-can-

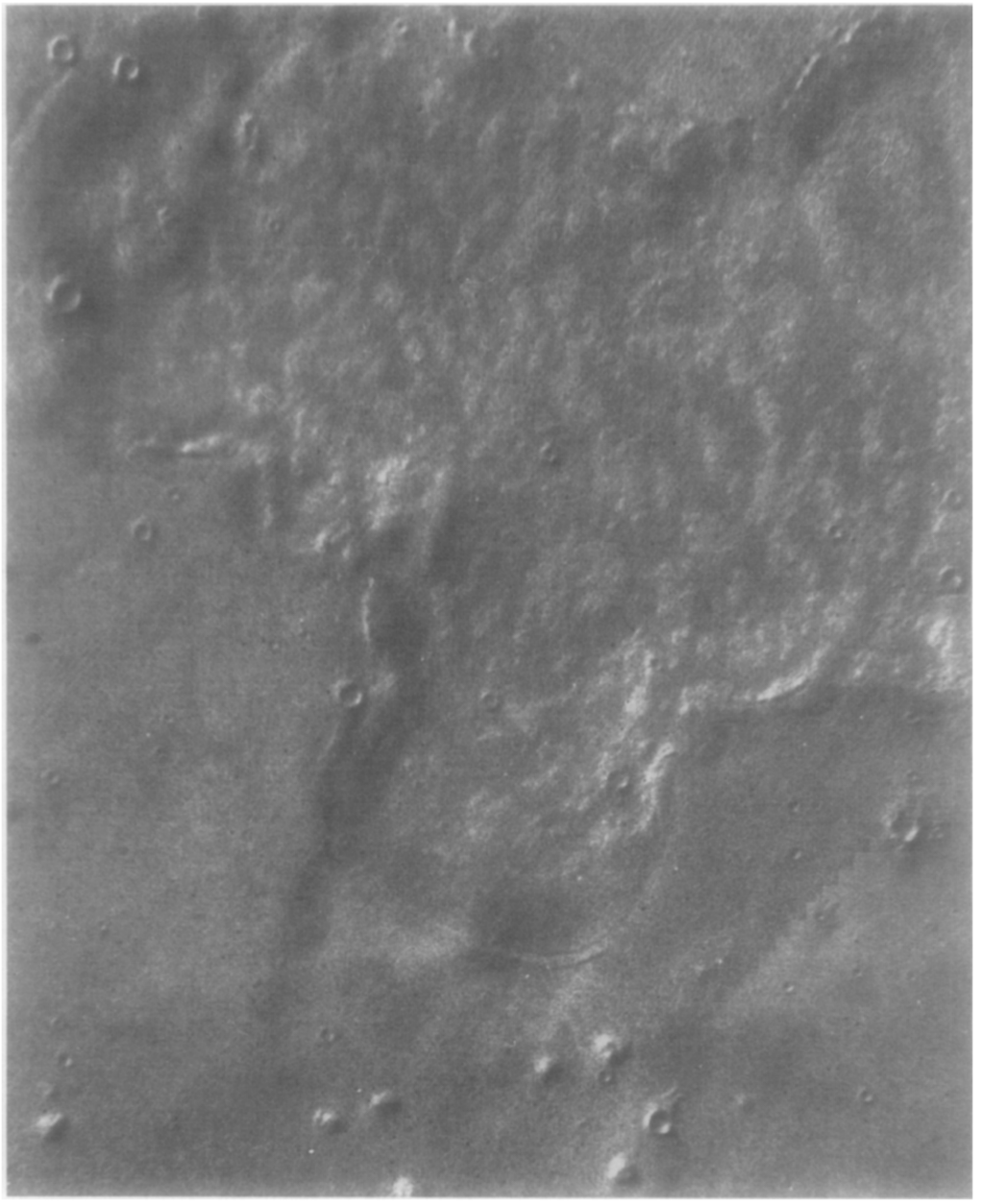

FIG. 11. High-resolution coverage of smooth, lobate contact between lowland units A and B across shallow fret trough (see Fig. 3 for location). The "thumbprint" terrain of unit B consists of numerous bright, low-relief mounds viewed against the relatively dark plains surface. Scene width, approximately 35 km. Viking Orbiter images: 52A38-40.

yon (northward). Individual mounds are typically ovate to elongate features up to 300 m across and as much as 3 km long (Figs. 8 and 11). The northern subunit consists of "mottled" plains, described by Carr (1981) and Witbeck and Underwood (1984). The mottled appearance is caused by the presence of numerous flow ejecta craters with bright ejecta blankets superposed on relatively dark plains (Carr 1981). The contact between these subunits typically is quite sharp (Fig. 12).

FIG. 12. High-resolution coverage of contact (arrowed) between striped or "thumbprint" terrain and mottled plains subunits of lowland unit B (see Fig. 3 for location). Scene width, approximately 65 km. Viking Orbiter images: 60A53,55,58.

Crater ages. Two crater populations were identified for lowland unit B. These correspond to crater retention ages from 4000 to 5500 and from 800 to 1400 (populations 1 and 2, respectively, Fig. 5). Population 1 appears similar in age to population 2 of both the cratered uplands and lowland unit A. Population 2 correlates well with population 3 of lowland unit A. Fitting the Neukum (1983) curve yields an age from 2200 to 4000 for population 1 (population 2 is the same as for a Neukum and Hiller 1981 fit). Like that of the cratered uplands, population 1 of unit B has a slope noticeably steeper than that of the Neukum (1983) production curve, but fits the Neukum and Hiller (1981) curve well. The oldest population of the cratered upland surface, partially preserved in lowland unit A, appears to be completely absent from unit B.

FRETTED TERRAIN

General Description

West Deuteronilus Mensae consists of extensive cratered upland "peninsulas" or plateaus cut by long, finger-like canyons typically 10 to 20 km wide and upwards of 300 km long. The longest of these canyons trend roughly north to northwest, approximately perpendicular to the lowland/upland boundary, and may indicate some local structural or topographic control. To the east of the study area (Fig. 2), dissection of the cratered uplands is more advanced, such that the highlands are expressed as isolated plateau remnants a few tens of kilometers or less across surrounded by smooth lowland plains (Lucchitta 1978). Much of southern Deuteronilus Mensae exhibits circular and arcuate escarpments that

likely indicate preferential degradation of buried large impact structures (Sharp 1973, Lucchitta 1978).

Detailed Description

The morphological changes in the fretted terrain across the gradational boundary in west Deuteronilus Mensae are typified by the fret canyon in Fig. 4. Cross-profiles of this canyon (Fig. 4c) exhibit up to five principal elements. These are: the plateau surface; the canyon wall; a slope intermediate in steepness between the canyon wall and the debris apron; the debris apron; and the canyon floor. The plateau and canyon floor surfaces appear to be essentially horizontal surfaces in all profiles. Slopes for the remaining three surfaces tend to decrease from south to north.

Canyon Adjacent to Cratered Uplands

Canyon walls. The total depth of the canyon within the cratered upland unit ranges from about 300 m just south of the contact between the cratered uplands and lowland unit A (Fig. 4), to more than 650 m south of Fig. 4. These values are significantly lower than those measured by Soderblom and Wenner (1978) and Carr (1986) for the fretted terrain to the east. The canyon walls are expressed as relatively steep cliffs (Figs. 13a–13c). The presence of shadows in places along the cliff (Figs. 13b and 13c) suggests slopes similar to the Sun elevation angle of 32° above the horizon for the very-high-resolution images. The cliffs comprise about 300 m of this depth in the south (Fig. 4c, profile E) to less than about 50 m of the total canyon depth at a point about 10 km south of the contact between the cratered uplands and lowland unit A (Fig. 4c, profile C). If this decrease in cliff height is projected northward, the cliff should wedge out between the upper plateau surface and the intermediate slope in the vicinity of the contact between the cratered uplands and lowland unit A. The base of the cliff, therefore, may be the expression of the contact between the cratered uplands and unit A on the canyon wall.

Intermediate slope. The intermediate slope is a gentler, smoother slope (Figs. 13a–13c). Comparing the medium- and very-high-resolution images of this surface on the canyon's east side (Fig. 13a) with that on the west side (Fig. 13b), suggests it has both a lower albedo and steeper slope than the adjacent debris aprons. This is borne out by the photoclinometric profiles of the same areas, which indicate slopes between 5 and 12° for this surface. This slope has been interpreted as a trough or "moat" between the canyon wall and the debris apron (Weiss and Fagan 1982). Although we interpret it as a sloped surface, we recognize that the upper apron margin appears elevated slightly above the base of the intermediate slope (Fig. 13a). A system of low ridges and swales, parallel to the cliff base, can be seen on this intermediate surface (Figs. 13a and 13b).

Debris aprons. The debris aprons occur as sharply defined, gently sloping surfaces whose distal margins are either concentric to isolated plateau outliers or parallel to canyon walls. They are typically less than 10 km wide and occur at the bases of all fret escarpments adjacent to the cratered uplands except those within a few tens of kilometers of the contact between the cratered uplands and lowland unit A (Fig. 3). Photoclinometric profiles support the observation that the aprons are convex in profile (Carr and Schaber 1977, Squyres 1978) with slopes averaging less than 5° (Fig. 4c). The aprons exhibit a complex, hummocky surface of small hills and hollows (Figs. 13a and 13b). The proximal and distal margins of the debris aprons are typically sharp in both medium- and very-high-resolution images (Fig. 4).

The complex surface morphology is absent on the debris apron surface to the north (Fig. 13c), though the distal margin of the apron is well defined in medium-resolution images. The northern limit of occurrence of prominent debris aprons lies just north of 45° latitude in this canyon (Fig. 4), about 40 km south of the contact between the cratered uplands and unit A. A similar

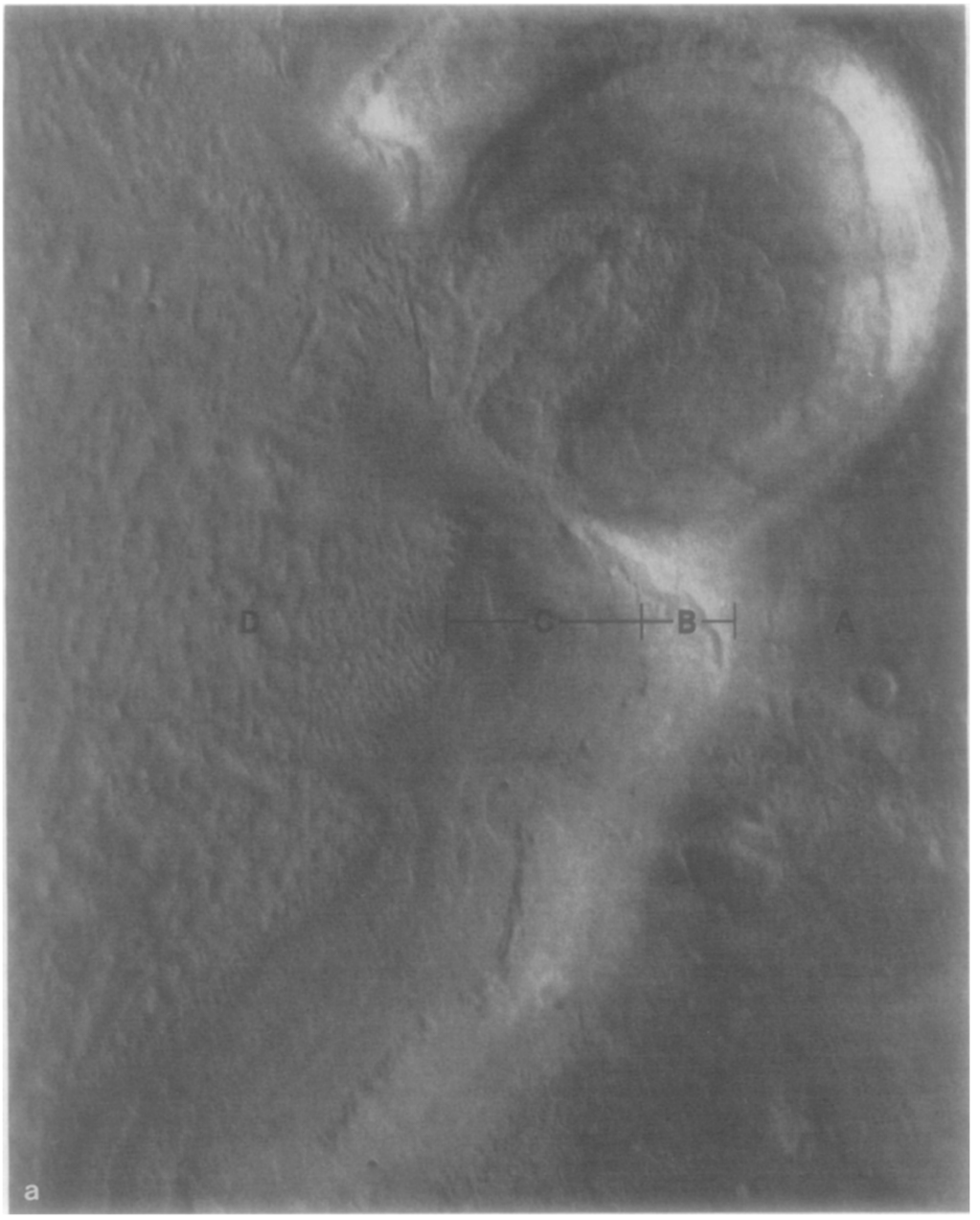

FIG. 13. Very-high-resolution detail of fret canyon adjacent to the cratered uplands (see Fig. 4 for locations). Plateau surface is indicated at A, canyon wall at B, intermediate slope at C and debris apron at D. (a) East side of fret canyon. Intermediate slope is separated from the canyon wall by a discontinuous bench, which can be identified within the breached 5-km crater at top right. Note the gentle ridge-and-swale structure parallel to the slope margins on the intermediate slope. The debris apron appears raised slightly above the base of the intermediate slope. Scene width, approximately 5 km. Viking Orbiter images: 458B45,46. (b) West side of fret canyon midway between (a) and (c). The canyon wall is narrower here than in (a). Ridges and swales, similar to those in (a), can be identified on the intermediate slope, but are discontinuous. Scene width, approximately 10 km. Viking Orbiter images: 458B47,48. (c) West side of fret canyon just south of contact between the cratered uplands and lowland

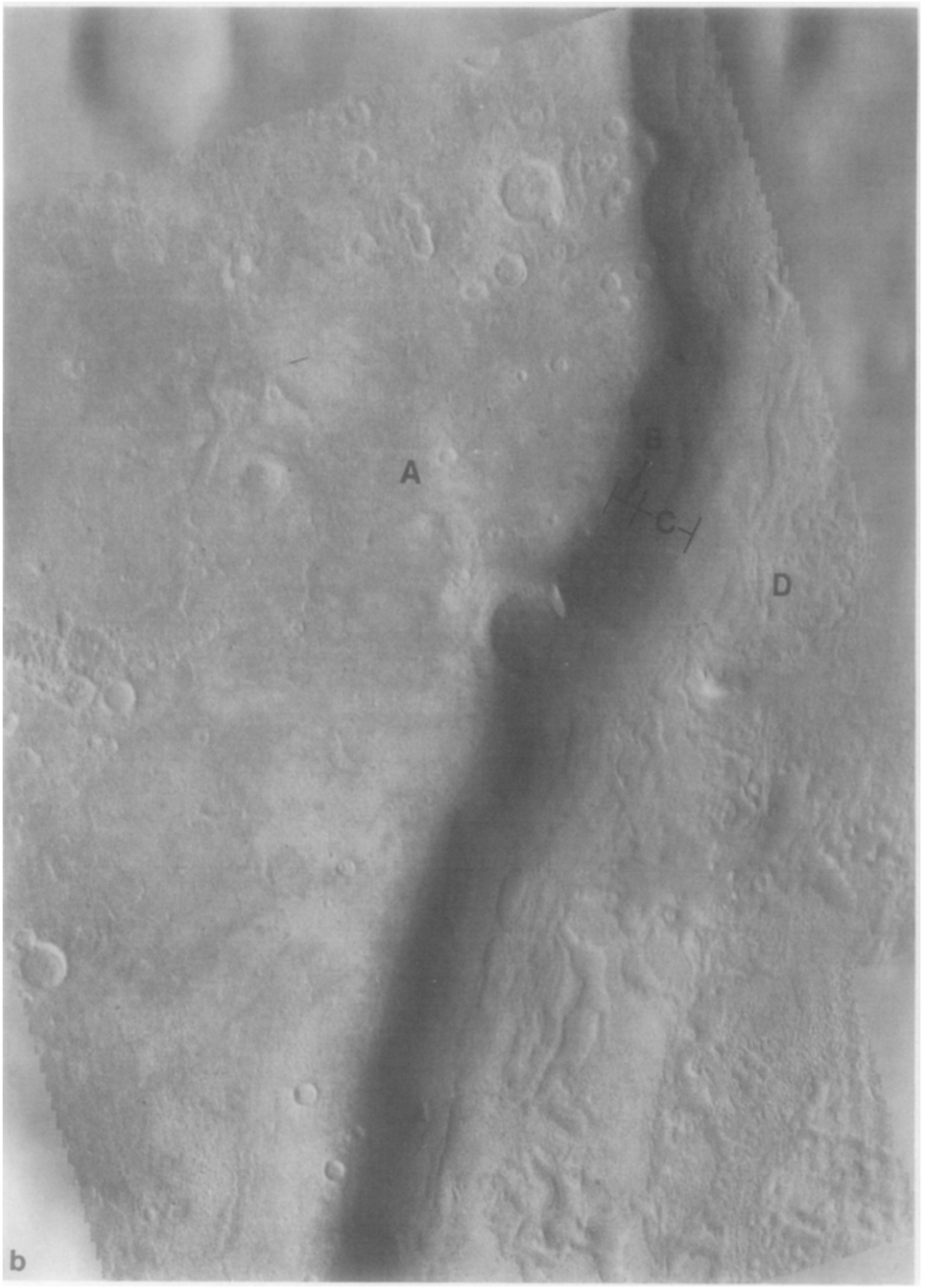

unit A. The cliff here is very narrow. The bench between the cliff and the intermediate slope may be the continuation of the contact between the cratered uplands and lowland unit A onto the canyon wall. The hummocky texture of the debris apron and the ridge-and-swale structure of the intermediate slope are absent in this area. The intermediate slope and debris apron both appear smooth. Scene width, approximately 10 km. Viking Orbiter images: 458B49,50.

FIG. 13—*Continued*

relationship occurs in other fret canyon reentrants (Fig. 3), though the distances vary somewhat. The canyon floors adjacent to the cratered uplands consist of smooth plains partially to completely buried by the debris aprons.

Canyon Adjacent to Lowland Unit A

Canyon walls. The total depth of the canyon adjacent to lowland unit A ranges from less than 200 m at the top of Fig. 4 to as high as about 300 m north of the contact between

the cratered uplands and unit A. The canyon walls here are less steep than are those adjacent to the cratered uplands (Fig. 4c). Slope estimates range from 9 to 22°, based on the presence and lack of true shadows in medium-resolution images with these Sun elevations. North of the escarpment at F, Fig. 4b, the walls do not exhibit true shadows in images with a Sun elevation of 9°. Using the photoclinometric profiles to further constrain these values yields wall slopes between 6 and 11°, in which the lower value corresponds to the wall toward the top of Fig. 4 and the higher value to the wall near the contact with the cratered uplands. These values are comparable to those of the intermediate slope to the south.

Perhaps the most interesting aspect of the canyon walls adjacent to lowland unit A is the presence of three or four parallel benches or breaks in slope (numbered 1 through 4, figs. 4, 8, and 14). Slope breaks 1 and 2 exhibit recognizable benches at very high resolution (Fig. 8). Shading across these benches suggests that the steepest elements of the slope profiles lie immediately above the benches, with the profile between benches having a convex upward shape. Benches 3 and 4 are defined by sharp breaks in slope (Fig. 14). Benches 1–3 are traceable for several kilometers along the canyon wall. Each bench occurs progressively higher up the canyon wall when traced from south to north (Fig. 4). Bench 1 defines the contact between lowland units A and B on the canyon wall.

Debris aprons. The debris aprons within lowland unit A are expressed as narrow, smooth, slopes about 1.5 km wide at the base of the canyon wall (Figs. 4, 8, and 14). Photoclinometric profiles suggest a slope averaging between 2 and 5° for this surface. The contact between this debris apron and the canyon floor is marked by a gradual change in slope and texture rather than by a prominent toe.

Canyon floor. The northern 30 km of canyon floor within lowland unit A covered by the very-high-resolution images (Figs. 4 and 8) is characterized by polygons similar to, but somewhat larger than, those to the northwest, and may indicate continuity of this surface onto the canyon floor.

DISCUSSION

Erosion of Regionally Stratified Material

The topographic relief of the fretted terrain provides compelling evidence that erosional retreat of the lowland/upland boundary has been a significant process. This erosion is generally thought to have involved sapping of interstitial ground ice or ground water at the cliff faces within the fretted terrain and transport of the material away from the cliffs down the fret canyons (Lucchitta 1984a, Sharp 1973, Sharp and Malin 1975, Squyres 1978, Carr 1980, 1986). However, fluvial transport of the material out of the fret canyons is insufficient to explain the advanced state of degradation of the upland terrain evident in the fretted terrain to the east (Lucchitta 1984a) and the lack of evidence of fluvial activity on the canyon floors.

One way to produce the lateral overlap of the fretted terrain by units associated with the gradational boundary might be through exposure of stratigraphic horizons by erosion. In this model, the cratered uplands, lowland unit A, and lowland unit B define lithologic units of regional extent that predate both the lowland/upland boundary and the fretted terrain. Unit B would be the oldest of the three.

The presence of parallel contacts separating units with easily recognizable albedo and morphologic differences on a slope is perhaps the most compelling reason to invoke an erosional stratigraphic model. The contacts trend up canyons and around plateau remnants in the fretted terrain just as would be expected of horizontal stratigraphic units exposed on an incised, sloping surface. Development of the lowland/upland boundary by this model requires two separate events: An erosional event to carve the fretted terrain; and an erosional or tectonic event to produce the broad,

FIG. 14. Very-high-resolution detailed view of west wall of fret canyon (see Fig. 4 for location). The plateau surface is labeled A; canyon wall, B; debris apron, C. Bench 2 and slope breaks 3 and 4 are numbered. "Bench" 2 is expressed as a gradual change in slope between the canyon wall and the debris apron in this part of the canyon. Scene width, approximately 10 km. Viking Orbiter image: 458B66.

sloping lowland/upland boundary surface. Though the scale of down-cutting implied by the fretted terrain is large, explaining it is not as difficult as accounting for erosion of the sloping lowland/upland boundary. Tectonic warping of the crust may provide an adequate explanation for the gross topography but would have warped stratigraphic horizons along with the surface.

Detailed examination of the unit contacts has revealed additional inconsistencies with a stratigraphic interpretation. If the contacts truly are stratigraphic contacts exposed by erosion, the cratered uplands should appear to onlap unit A and unit A should onlap unit B, never the other way around. Continuity of stratigraphic contacts across degraded crater floors implies deposition after formation of the crater instead of erosion, since the impact would have disrupted a stratified target.

Differential erosion of resistant strata is probably the most common terrestrial example of bench morphology. Stratigraphic units with high erosional resistance tend to be cliff formers. In a cross-profile of a slope of this type, benches lie at the tops of cliffs and the profile shape between benches is concave upward. The concave slope is produced by accumulation of debris wasted from the cliff. In contrast, the west Deuteronilus Mensae benches 1 and 2 exhibit the opposite shape and bench position. Stratigraphic benches are more likely to be well expressed where slopes are greatest, so that debris wasted from the slope can be easily removed. Benches 1–3 in west Deuteronilus Mensae all lie on gentle slopes.

A stratigraphic interpretation is further complicated by a need to explain the crater densities for the three units (Fig. 5). If the gradational lowland/upland boundary surface had been produced by a single erosional event, crater populations should reflect the timing of the event, rather than the age of the stratigraphic units, and therefore exhibit a single crater age. The fretted terrain represents an additional erosional event and should therefore exhibit a second, lower crater density. But because the lowland units display distinct crater densities, formation of the gradational boundary by this model requires the unlikely sequence of separate erosional events affecting only those surfaces below a given stratigraphic boundary or exhumation of previously cratered surfaces.

If lowland units A and B had been buried before their surfaces had accumulated many craters and later exhumed, they might exhibit lower crater densities than the overlying cratered upland material. But craters within the lowland units tend to be more pristine than those within the cratered uplands. The exhumation process would have to have removed the overlying mateial without degrading the exhumed craters. Population 1 of lowland unit A (Fig. 5), which appears to be a remnant of population 1 of the cratered uplands, cannot be explained by this model. The most difficult problem to overcome, however, is that exhumation implies removal of the overlying cratered upland and lowland unit A material from the entire northern lowlands. Redeposition of so much material would be difficult to account for with known deposits elsewhere on the planet, even if a suitable exhumation mechanism could be found.

Removal of interstitial ice through sublimation resulting in scarp retreat has been suggested as a mechanism by which the contact between lowland units A and B and the striped appearance of unit B might have developed (e.g., Carr and Schaber 1977, Rossbacher 1985). This ice might have been present throughout the Martian megaregolith prior to formation of the global dichotomy (Carr and Clow 1981, Clifford 1980, Sharp 1973, Soderblom and Wenner 1978, Soderblom *et al.* 1973) or it may have been emplaced through volatile-rich eolian sedimentation (Grizzaffi and Schultz 1987, Soderblom *et al.* 1973) or ice-rich outflow channel sedimentation (e.g., Carr 1981, Guest *et al.* 1977, McGill 1985, 1986). However, the contact between the two units

does not always coincide with an escarpment. Subdued plateau outliers may lie several tens of kilometers north of the contact between units A and B, their surfaces being composed solely of unit B material. The escarpments, therefore, likely indicate fretted terrain that predates emplacement of lowland units A and B.

Plains Emplacement

Eolian Deposition

There is abundant evidence in the form of wind streaks and vast dune fields that indicates that eolian sediments may be present over much of the northern plains (Breed *et al.* 1979, Grizzaffi and Schultz 1987, Thomas 1982, Soderblom *et al.* 1973, Ward 1979). Analysis of Viking Orbiter images has revealed that many of these features are currently active, or at least in equilibrium with Martian global wind circulation (Thomas 1982). Could lowland units A and B represent successive eolian loess blankets onlapping the cratered upland margin? Because both units are cratered, whereas the wind streaks and dunes are not, they would have to be relatively old, stabilized deposits to avoid their redistribution by recent Martian wind activity.

The boundaries of the two plains units are difficult to produce with an eolian model. An eolian blanket would probably thin gradually toward its margin, resulting in a diffuse contact whose placement would be subject mainly to available image resolution (Zimbelman 1987). Even more important, eolian deposits are not gravitationally confined as are fluids like low-viscosity lavas or water, and therefore would not likely produce a topographically conformal contact.

Volcanism

Emplacement of volcanic plains similar to the lunar mare basalts within the northern lowlands has been suggested by a number of investigators (e.g., Carr 1981, Wise *et al.* 1979, Theilig and Greeley 1979). Very-large-scale, lunar-like volcanic plains emplacement might be expected during, and immediately following, the planet's accretionary phase. This is implied by the model of Wise *et al.* (1979), in which the gross resurfacing of the northern lowlands took place very early, though the present plains surfaces may reflect subsequent emplacement processes. Carr (1981) and Theilig and Greeley (1979) conclude that the northern plains, in the lower latitudes at least, are volcanic, based on the presence of wrinkle ridges similar to those found within the lunar mare. Recent work by Plescia and Golombek (1986), however, shows that terrestrial wrinkle ridge analogs indicate compressional stress environments in a variety of materials, including sediments, with a range of rheologies.

Continuity of the contact between the cratered uplands and lowland unit A onto the wall of the canyon in Fig. 4 would require emplacement of a lava shoreline after formation of the fretted terrain. High stands of lava lakes do not appear reasonable given the great extent of the northern lowlands. To create lava shorelines in the conventional way, recession of the lava lake surface is required. Plains volcanism on a scale sufficient to flood most of the northern plains would require tremendous volumes of lava, even when compared to other examples of planetary volcanism, relatively late in Martian geologic history. Large flood basalt deposits on the Earth, such as the Columbia River Basalts, can be of the order of hundreds of meters thick, but are composed of many individual units that are typically less than a few tens of meters thick (e.g., Williams and McBirney 1979, Mackin 1971). The volumes for these basaltic floods, though quite large, are still several orders of magnitude smaller than those required to produce shorelines along the periphery of the northern plains of Mars. While lunar lava shorelines or marginal terraces (Wilhelms 1987) bear a weak resemblance to these benches, they do not appear to involve so great a reduction in height of the lava surface. Further, lunar (and other Martian) volcanic plains do not generally

preserve much of the underlying topography, but the fretted terrain north of the gradational boundary is easily identified. The smooth, arcuate morphology along the lower contact separating lowland units A and B does not compare well with the more irregular, lobate morphology typical of lava flow fronts and is not found at lunar plains boundaries.

The polygonal surface texture within lowland unit A could be interpreted as due to cooling cracks on lava lakes (Carr and Greeley 1980), though terrestrial examples rarely exceed several meters across. The bright, low mounds within the striped unit of lowland unit B might be interpreted as volcanic extrusions of material with an albedo higher than that of the surrounding plains (Frey and Jarosewich 1982), but their great numbers and arcuate distributions are difficult to explain in a volcanic context.

The general decrease in crater densities from cratered uplands through lowland unit B is consistent with volcanic plains emplacement onto the sloping upland surface. The depth of crater burial should be greater to the north, leading to progressively lower crater densities from south to north. Fitting the crater populations for the 3 units to either the Neukum and Hiller (1981) or the Neukum (1983) curve does not affect this trend.

Deposition in Standing Water

Repeated inundation of the northern lowlands by floods associated with outflow channel development elsewhere along the lowland/upland boundary is an alternative mechanism capable of producing the topographically conformal contacts and the draped appearance of the fretted terrain. Lowland units A and B, by this model, represent cratered uplands and fretted terrain that has been reworked and draped with lake sediments. Lowland unit B represents the latest and least extensive of the two plains-flooding episodes.

The volume of water required to flood the northern lowlands is consistent with many models of global water inventories (e.g., Anders and Owen 1977, Carr 1986, Fanale *et al.* 1982, Kahn 1985, Pollack 1979, 1986, Pollack and Black 1979, Rasool and Le Sergeant 1977, Toon *et al.* 1980) and is implied by the 35-m global equivalent estimate of Carr (1986) for the amount of water involved in the formation of the circum-Chryse outflow channels. Confined to the northern lowland plains, approximately 25% or less of the planet's surface (excluding Tharsis and Alba Patera, the Elysium volcanics and the polar cap) yields an average depth of over 100 m of water from this single event. It is difficult to imagine this much water, discharged catastrophically, soaking into the ground or evaporating rapidly enough to avoid accumulating, at least temporarily, in some form of large body of standing water. Lucchitta *et al.* (1986) proposed sediment deposition in an ice-covered ocean to explain the presence of apparently thick sediments within the lowlands (the large-scale polygonal terrains) and the lack of recognizable alluvial fan morphology at outflow channel mouths. We would add that the boundary morphologies we have observed may require multiple floods into the lowland plains with temperatures above freezing long enough to enable the development of lacustrine shoreline morphology.

The distribution of the unit contacts and their relationships to pre-existing terrain are consistent with a shoreline interpretation. The southward offset of the contacts between units within the fret canyons indicates embayment of the canyons. Plateau outliers crossed by unit contacts may have been partially submerged on their lower north sides. Contacts crossing degraded crater floors can be explained as embayment of the craters. The ultimate elevation attained by a body of standing water is less limited than that of a lava lake, simply because tens or hundreds of meters of water can subsequently be removed more easily than can lava.

Strandlines may consist of both benches or shore platforms (Bradley 1958) and

beach ridges depending on whether material is being removed or deposited at a particular location. This may be the only terrestrial analog process that can produce boundaries that exhibit both erosional and depositional structures and that conform to topography over broad regions. Terrestrial lakeshore platforms can also exhibit profiles (e.g., Reeves 1968) similar to those observed for benches 1 and 2 (Figs. 4c and 8) and the contact between the cratered uplands and lowland unit A in Figs. 13a–13c. Beach ridges are constructional features that may be several meters in height, tens of meters in width, and hundreds of meters to kilometers in length (Reineck and Singh 1980). Multiple beach ridges can exhibit ridge-and-swale topography similar to that observed along the contact between lowland units A and B on the floor of the fret canyon in Fig. 4. This feature (and the similar feature in Fig. 11) bears a strong resemblance to beach ridges and bars of the north Lake Bonneville region of Utah (Fig. 15). The arcuate patterns are caused by wave refraction (e.g., Zenkovich 1967).

The lack of prominent debris aprons in the fretted terrain adjacent to lowland units A and B may be a result of reworking or complete removal of the debris by waves as the shoreline advanced or receded. Formation of the debris aprons themselves may have been aided by rising and falling water levels. The removal of debris wasted and/or sapped from the fret canyon walls in a near-shore lacustrine environment would be efficient and could produce the smooth canyon floor surfaces without affecting the plateau surface. Near-shore lacustrine erosion provides a very effective way of maintaining cliffs by focusing erosion at the bases of the cliffs and preventing the accumulation of talus deposits.

The polygons in northern lowland unit A and the bright low mounds in the striped plains of unit B may be more easily explained in a lacustrine than in a volcanic context. Both giant desiccation polygons and ice-wedge polygons form in lacustrine or coastal marine environments (Lachenbruch 1962, Leffingwell 1915, Mackay 1973, 1986). Desiccation polygons up to several tens of meters across are common on playa surfaces in the Great Basin of the American southwest (Motts and Carpenter 1968, Reeves 1968). Ice-wedge polygons up to several tens of meters across are very common in the Arctic coasts of northern Canada and Alaska (Black 1974, Leffingwell 1915, Mackay 1973, 1986). Ice wedges between polygons are typically less than a few meters wide, though very large, buried ice wedges may be as large as 10 m wide (Billings and Peterson, 1979). Ice wedges indicate thermal expansion and contraction in frozen ground and grow as a result of the introduction of liquid water or snow into thermal cracks that form in the ice during winter (Billings and Peterson 1979, Black 1974, Mackay 1986).

The bright, low-relief mounds are similar to frost heave structures in freezing wet sediments. Similar dome-like hills elsewhere within the lowland plains may be pingos (e.g., Lucchitta 1981, Rossbacher and Judson 1981). Mackenzie delta-type pingos are common structures in the Canadian Arctic that form as water is concentrated in lenses below a downward aggrading permafrost zone in recently drained lakes (Mackay 1962, 1973). These lenses tend to develop in sediments with relatively high permeabilities, particularly sandy sediments. The tendency for the bright mounds to form arcs parallel to the contact between lowland units A and B in the fret canyons might indicate ice concentration along former beach sand ridges that were formed and later buried by finer lake sediments during shoreline advance. The bright pits may be deflated mounds. Deflation of the mounds suggests that they consist of friable, entrainable materials. Sublimation of a pingo ice core would contribute to its removal.

The low crater densities in lowland units A and B could have been produced by sediment deposition onto and reworking of the

FIG. 15. Aerial photographic mosaic of part of the Lake Bonneville region of Utah. Numerous arcuate ridges are beach ridges and bars associated with changing lake levels. The largest of these bars are over 15 km long. Compare these features with the contact between lowland units A and B in Figs. 8 and 11. Scene width, approximately 50 km. North is toward the bottom of the frame. Aerial photographs courtesy of Eros Data Center.

old cratered upland surface. Burial and reworking of cratered terrain by lake sedimentation and wave action should produce progressively lower crater densities from south to north as would burial by volcanic plains. It would therefore appear that, while comparison of the crater population curves may point to plains emplacement

rather than exhumation, it is not sufficient to pin down the emplacement process by itself.

Questions raised by a lacustrine or shallow marine interpretation are largely related to estimates of the volume of water responsible for carving the outflow channels and our present understanding of the Martian paleoclimate. Models of the early Martian climate are dependent upon a number of complexly interrelated geochemical, climatological, and astronomical factors. Chief among these are the CO_2, H_2O, and other volatile inventories which determine the mass and greenhouse warming of the early atmosphere. Current estimates of the amount of outgassed CO_2 during Mars' history range from a minimum of a few hundred millibars to 3 bars (e.g., Rasool and Le Sergeant 1977, Anders and Owen 1977, Pollack and Black 1979) to as much as 10 to 20 bars (Carr 1986). In Carr's 1986 model, the atmospheric pressure due to CO_2 may not have exceeded more than a few bars at any given time since outgassing likely was protracted over a long period and since carbonate rocks may have formed relatively rapidly in the presence of liquid water (Fanale *et al.* 1982, Kahn 1985). Estimates of the outgassed H_2O inventory vary from as low as the equivalent of a few meters to several hundred meters or more averaged globally (Carr 1986, Pepin 1986). CO_2 pressures required to maintain average global temperatures, or at least seasonal equatorial temperatures, above freezing range from at least a few hundred millibars, assuming the most favorable conditions and a present solar luminosity (Toon *et al.* 1980), to 3 bars or more (Pollack 1979, 1986). Postawko and Kuhn (1986), however, doubted that above freezing temperatures could be achieved due the 20–30% lower solar luminosity in Mars' early history even with the higher assumed pressures, unless brines (Zent and Fanale 1985) were postulated.

To produce beach morphology at scales sufficient for recognition in Viking Orbiter images requires temperatures and atmospheric pressures high enough to allow surface waves. Lacustrine features at comparable scales in the Lake Bonneville area of Utah and Nevada typically formed within a few thousand years or less (Currey 1980). The time required to produce similar features on Mars would depend on the composition of the surface material and its resistance to erosion, and the available wind-driven wave energy. This time requirement could be significantly reduced if the preexisting terrain had not been subject to frequent shoreline advances. Some large-scale depositional features in Lake Bonneville apparently formed relatively rapidly during the initial transgression, when the preexisting surface was in maximum disequilibrium with shore-zone processes (Currey 1980).

CONCLUSIONS

The implications of the lateral overlap of the fretted terrain boundary by the gradational boundary in west Deuteronilus Mensae are twofold. First, the two major unit contacts may represent stratigraphic contacts that were exposed by development of the sloping upland margin and dissection of it by formation of the fretted terrain. Second, the contacts may define the margins of plains emplaced onto the preexisting fretted terrain and the sloping upland margin.

I. Erosion of Stratified Upland Terrain

1. The gradational boundary southwest of Deuteronilus Mensae requires an erosional mechanism that can produce the sloping upland margin on a regional scale and another, later event to carve the fretted terrain. Superpositional relationships in west Deuteronilus Mensae are opposite to what would be expected if the gradational boundary were strictly an erosional feature. Stratigraphic benches would not likely be as well preserved on gentle slopes as on steep slopes where debris can more easily be removed. Benches in west Deuteronilus Mensae are best defined on the gentle slopes.

2. Crater densities decrease plainward across the gradational boundary and are distinct for each unit, requiring separate erosional events to produce lowland units A and B, or exhumation of lightly cratered lowland plains. The scale of erosion implied by either process may be too large to account for with known deposits elsewhere on the planet.

II. Plains Emplacement onto Sloping Upland Margin and Fretted Terrain

1. Eolian sediment deposition onto the sloping upland margin and fretted terrain would not likely produce sharp, topographically conformal contacts.

2. Plains volcanism requires that the lava recede vertically by hundreds of meters within the northern lowlands in order to produce lava shorelines high on the canyon walls in the fretted terrain and not obscure the underlying fretted terrain.

3. We feel that sediment deposition in either a liquid or ice-covered sea provides the best explanation for the observed boundary relationships. Many of the observed morphologies resemble those found along terrestrial lake shores in cold environments. These include shore features such as wave terraces, beach ridges, and arcuate or cuspate patterns and coastal plains features such as desiccation or ice-wedge polygons and pingos.

Transient large bodies of standing water within the northern lowlands represent a plausible outcome of catastrophic flooding elsewhere along the lowland/upland boundary, particularly when the tremendous scale of the circum-Chryse and Elysium outflow channels is considered. The volume of water required to flood the lowland plains appears consistent with estimates of Martian global water inventories. Temperatures and atmospheric pressures sufficient to allow large bodies of liquid water to remain stable at least temporarily may have been required relatively late in Martian history.

ACKNOWLEDGMENTS

The authors thank Drs. Larry Soderblom and Jeff Plescia of the United States Geological Survey, Astrogeology Branch, Flagstaff, Arizona, for their assistance with the photoclinometry. We also thank Drs. Stephen Baloga and David Pieri for reviewing the manuscript and providing helpful comments. This work was carried out at the Jet Propulsion Laboratory, California Institute of Technology, under contract with the National Aeronautics and Space Administration.

REFERENCES

Anders, E., and T. Owen 1977. Mars and Earth: Origin and abundance of volatiles. *Science* **198,** 453–465.

Billings, W. D., and K. M. Peterson 1979. Vegetational change and ice-wedge polygons through the thaw–lake cycle, arctic Alaska. Report prepared for the National Science Foundation, Washington, DC, Division of Polar Programs, U. S. Department of Commerce, National Technical Information Service. Report PB80-147911.

Black, R. F. 1974. Ice-wedge polygons of northern Alaska. In *Glacial Geomorphology* (D. R. Coates, Ed.), pp. 247–275. Publications of Geomorphology, State University of New York, Binghamton.

Bradley, W. C. 1958. Submarine abrasion and wave-cut platforms. *Geol. Soc. Amer. Bull.* **69,** 967–974.

Breed, C. S., M. J. Grolier, and J. F. McCauley 1979. Morphology and distribution of common "sand" dunes on Mars: Comparison with the Earth. *J. Geophys. Res.* **84,** 8183–8204.

Carr, M. H. 1980. The morphology of the Martian surface. *Space Sci. Rev.* **25,** 231–284.

Carr, M. H. 1981. *The Surface of Mars.* Yale Univ. Press, New Haven, CT/London.

Carr, M. H. 1984. Mars. In *Geology of the Terrestrial Planets,* pp. 207–263. NASA SP-469.

Carr, M. H. 1986. Mars: A water-rich planet? *Icarus* **68,** 187–216.

Carr, M. H., and G. D. Clow 1981. Martian channels and valleys: Their characteristics, distribution, and age. *Icarus* **34,** 91–117.

Carr, M. H., and R. Greeley 1980. *Volcanic Features of Hawaii—A Basis for Comparison with Mars.* NASA SP-403.

Carr, M. H., and G. G. Schaber 1977. Martian permafrost features. *J. Geophys. Res.* **82,** 4039–4054.

Clifford, S. M. 1980. Mars: Ground ice replenishment from a subpermafrost ground water system. In *Proceedings 3rd Colloquium on Planetary Water, State University of New York, Buffalo,* pp. 68–75.

Currey, D. R. 1980. Coastal geomorphology of Great Salt Lake and vicinity. *Utah Geol. Mineral Survey Bull.* **116,** 69–82.

Fanale, F. P., J. R. Salvail, W. B. Banerdt, and

R. S. SAUNDERS 1982. The regolith–atmosphere–cap system and climate change. *Icarus* **50,** 381–407.

FREY, H., AND M. JAROSEWICH 1982. Subkilometer Martian volcanoes—Properties and possible terrestrial analogs. *J. Geophys. Res.* **87,** 9867–9879.

FREY, J., B. L. LOWRY, AND S. A. CHASE 1979. Psuedocraters on Mars. *J. Geophys. Res.* **84,** 8075–8086.

FREY, H., AND J. SEMENIUK 1988. Extent of buried cratered terrain underlying the highland/lowland transition zone in eastern Mars. *Lunar Planet. Sci. XIX,* 360–361. Lunar Planet. Inst., Houston, TX.

FREY, H., A. M. SEMENIUK, J. A. SEMENIUK, AND S. TOKARCIK 1986. Crater counts in the transition zone in eastern Mars: Evidence for common resurfacing events. *Lunar Planet. Sci. XVII,* 243–244. Lunar Planet. Inst., Houston, TX.

GRANT, T. D., AND H. FREY 1988. Resurfacing events in the Lunae Planum–Xanthe Terra region of Mars. *Lunar Planet. Sci. XIX,* 413–414. Lunar Planet. Inst., Houston, TX.

GRANT, T. D., H. FREY, AND J. A. SEMENIUK 1988. Resurfacing events in the Tempe Terra region of Mars. *Lunar Planet. Sci. XIX,* 415–416. Lunar Planet. Inst., Houston, TX.

GREELEY, R., AND J. E. GUEST 1987. Geologic Map of the Eastern Equatorial Region of Mars. USGS Map I-1802-B, Atlas of Mars, 1:15,000,000 Geologic Series.

GRIZZAFFI, P., AND P. H. SCHULTZ 1987. Isidis Basin: Site of ancient volatile-rich debris layer. *Icarus* in press.

GUEST, J. E., P. S. BUTTERWORTH, AND R. GREELEY 1977. Geological observations in the Cydonia region of Mars from Viking. *J. Geophys. Res.* **82,** 4111–4120.

KAHN, R. 1985. The evolution of CO_2 on Mars. *Icarus* **62,** 175–190.

LACHENBRUCH, A. H. 1962. *Mechanics of Thermal Contraction Cracks and Ice-Wedge Polygons in Permafrost.* Geol. Soc. Amer., Spec. Paper 70.

LEFFINGWELL, E. DEK. 1915. Ground-ice wedges: The dominant form of ground-ice on the north coast of Alaska. *J. Geol.* **23,** 635–654.

LUCCHITTA, B. K. 1978. Geologic Map of the Ismenius Lacus Quadrangle of Mars. USGS Map I-1065, Atlas of Mars, 1:5,000,000 Geologic Series.

LUCCHITTA, B. K. 1981. Mars and Earth: Comparison of cold-climate features. *Icarus* **45,** 264–303.

LUCCHITTA, B. K. 1984a. Ice and debris in the fretted terrain, Mars. *J. Geophys. Res.* **89,** B409–B418.

LUCCHITTA, B. K. 1984b. Small-scale polygons on Mars. *Rep. Planet. Geol. Prog.—1983,* pp. 205–207. NASA TM 86246.

LUCCHITTA, B. K., H. M. FERGUSON, AND C. SUMMERS 1986. Sedimentary deposits in the northern lowland plains, Mars. *J. Geophys. Res.* **91,** E166–E174.

MACKAY, J. R. 1962. Pingos of the Pleistocene MacKenzie Delta area. *Geog. Bull.* **18,** 21–63.

MACKAY, J. R. 1973. The growth of pingos, western Arctic coast, Canada. *Canad. J. Earth Sci.* **10,** 979–1004.

MACKAY, J. R. 1986. The first seven years (1978–1985) of ice-wedge growth, Illisarvik experimental drained lake site, western Arctic coast. *Canad. J. Earth Sci.* **23,** 1782–1795.

MACKIN, J. H. 1971. *Stratigraphic Section in the Yakima Basalt . . . in South Central Washington.* Report of Investigations—19, Division of Mines and Geology, State of Washington.

MAXWELL, T. A., AND G. E. MCGILL 1988. Ages of fracturing and resurfacing in the Amenthes region, Mars. *Proc. Lunar Planet. Sci. XVIII,* 701–711. Lunar Planet. Inst., Houston, TX/Cambridge Univ. Press, New York/London.

MCGILL, G. E. 1985. Age and origin of large martian polygons. *Lunar Planet. Sci. XVI,* 534–535. Lunar Planet. Inst., Houston, TX.

MCGILL, G. E. 1986. The giant polygons of Utopia, northern martian plains. *Geophys. Res. Lett.* **13,** 705–708.

MOTTS, W. S., AND D. CARPENTER 1968. Report of test drilling on Rogers, Coyote, Rosamond, and Panamint Playas in 1966. In *Geology, Mineralogy, and Hydrology of U. S. Playas,* Chap. 3, pp. 32–57. AFCRL Report N68-27354.

MUTCH, T. A., R. E. ARVIDSON, J. W. HEAD, K. L. JONES, AND R. S. SAUNDERS 1976. *The Geology of Mars.* Princeton Univ. Press, Princeton, NJ.

NEUKUM, G. 1983. *Meteoritenbombardment und Datierung Planetarer Oberflachen.* Habilitationsschrift, Ludwig-Maximilians-Universitat, Munich.

NEUKUM, G., AND K. HILLER 1981. Martian ages. *J. Geophys. Res.* **86,** 3097–3121.

PEPIN, R. O. 1986. Volatile inventory of Mars. In *Symposium on Mars: Evolution of Its Climate and Atmosphere,* pp. 86–87. Lunar Planet. Inst., Houston, TX.

PIERI, D. C. 1980. *Geomorphology of Martain Valleys.* NASA Technical Memo 81979.

PLESCIA, J. B., AND M. GOLOMBEK 1986. Origin of planetary wrinkle ridges based on the study of terrestrial analogs. *Geol. Soc. Amer. Bull.* **97,** 1289–1299.

POLLACK, J. B. 1979. Climate change on the terrestrial planets. *Icarus* **37,** 479–533.

POLLACK, J. B. 1986. Longevity of a dense carbon dioxide atmosphere on Mars. In *Workshop on the Evolution of the Martian Atmosphere,* p. 37. Lunar Planet. Inst. Tech. Report 86-07, Lunar Planet. Inst., Houston, TX.

POLLACK, J. B., AND D. C. BLACK 1979. Implications of the gas compositional measurements of Pioneer Venus for the origin of planetary atmospheres. *Science* **205,** 56–59.

POSTAWKO, S. E., AND W. R. KUHN 1986. Effect of the greenhouse gasses (CO_2, H_2O, SO_2) on martian paleoclimate. *J. Geophys. Res.* **91,** D431–D438.

RASOOL, S. I., AND L. LE SERGEANT 1977. Implications of the Viking results for volatile outgassing from Earth and Mars. *Nature* **266,** 822–823.

REEVES, C. C., JR. 1968. *Introduction to Paleolimnology*. Elsevier, Amsterdam/London/New York.

REINECK, H. E., AND I. B. SINGH 1980. *Depositional Sedimentary Environments, with Reference to Terrigenous Clastics*. Springer-Verlag, Berlin/Heidelberg/New York.

ROSSBACHER, L. A. 1985. Ground ice models for the distribution and evolution of curvilinear landforms on Mars. In *Models in Geomorphology* (Woldenberg, Ed.), pp. 343–372. Allen & Unwin, Boston.

ROSSBACHER, L. A., AND S. JUDSON 1981. Ground ice on Mars: Inventory, distribution, and resulting landforms. *Icarus* **45,** 39–59.

SCOTT, D. H., AND M. H. CARR 1978. Geologic Map of Mars. USGS Map I-1083, Atlas of Mars, 1:25,000,000 Geologic Series.

SCOTT, D. H., AND K. L. TANAKA 1986. Geologic Map of the Western Equatorial Region of Mars. USGS Map I-1802-A, Atlas of Mars, 1:15,000,000 Geologic Series.

SHARP, R. P. 1973. Mars: Fretted and chaotic terrains. *J. Geophys. Res.* **78,** 4073–4083.

SHARP, R. P., AND M. C. MALIN 1975. Channels of Mars. *Geol. Soc. Amer. Bull.* **86,** 593–609.

SODERBLOM, L. A., T. J. KRIEDLER, AND H. MASURSKY 1973. Latitudinal distribution of a debris mantle on the martian surface. *J. Geophys. Res.* **78,** 4117–4122.

SODERBLOM, L. A., AND D. B. WENNER 1978. Possible fossil H_2O liquid–ice interfaces in the Martian crust. *Icarus* **34,** 622–637.

SQUYRES, S. W. 1978. Martian fretted terrain: Flow of erosional debris. *Icarus* **34,** 600–613.

SQUYRES, S. W. 1979. The distribution of lobate debris aprons and similar flows on Mars. *J. Geophys. Res.* **84,** 8087–8096.

TANAKA, K. L. 1986. The stratigraphy of Mars. *Proc. Lunar Planet. Sci. XVII.* In *J. Geophys. Res.* **91,** E139–E158.

TANAKA, K. L., AND D. H. SCOTT 1987. Geologic Map of the Polar Regions of Mars. USGS Map I-1802-C, Atlas of Mars, 1:15,000,000 Geologic Series.

THEILIG, E. AND R. GREELEY 1979. Plains and channels in the Lunae Planum–Chryse Planitia region of Mars. *J. Geophys. Res.* **84,** 7994–8010.

THOMAS, P. 1982. Present wind activity on Mars: Relation to large latitudinally zoned sediment deposits. *J. Geophys. Res.* **87,** 9999–10008.

TOON, O. B., J. B. POLLACK, W. WARD, J. A. BURNS, AND K. BILSKI 1980. The astronomical theory of climatic change on Mars. *Icarus* **44,** 552–607.

WARD, A. W. 1979. Yardangs on Mars: Evidence of recent wind erosion. *J. Geophys. Res.* **84,** 8147–8166.

WEISS, D., AND J. J. FAGAN 1982. Possible evidence of hydrocompaction within the fretted terrains of Mars. *Rep. Planet. Geol. Prog.— 1982,* pp. 239–241. NASA Tech. Memo 85127.

WEISS, D., J. J. FAGAN, J. STEINER, AND O. L. FRANKE 1981. Preliminary observations of the detailed stratigraphy across the highland–lowlands boundary. *Rep. Planet. Geol. Prog.—1981,* pp. 422–425. NASA TM 84211.

WILHELMS, D. E. 1987. *The Geologic History of the Moon*. USGS Prof. Paper 1348.

WILLIAMS, H., AND A. R. MCBIRNEY 1979. *Volcanology*. Freeman, Cooper, San Francisco.

WISE, D. U., M. P. GOLOMBEK, AND G. E. MCGILL 1979. Tectonic evolution of Mars. *J. Geophys. Res.* **84,** 7934–7939.

WITBECK, N. E., AND J. R. UNDERWOOD, JR. 1984. Geologic Map of the Mare Acidalium Quadrangle, Mars, rev. Map I-1614, USGS Atlas of Mars, 1:5,000,000 Geologic Series.

ZIMBELMAN, J. R. 1987. Spatial resolution and the geologic interpretation of martian morphology: Implication for subsurface volatiles. *Icarus* **71,** 257–267.

ZENKOVICH, V. P. 1967. *Processes of Coastal Development* (J. A. Steers, Ed.). Wiley–Interscience, New York.

ZENT, A. P., AND F. P. FANALE 1985. Solis Lacus brines: Possible chemistry and kinetics. *Lunar Planet. Sci. XVI,* 930–931. Lunar Planet. Inst., Houston, TX.